Heaven's Light is Our Guide

Department of Electronics & Telecommunication Engineering

Rajshahi University of Engineering & Technology, Bangladesh

Numerical Study of Surface Plasmon Resonance Biosensor Employing Bismuth Ferrite, Black Phosphorus and Zinc Telluride for Blood Group Detection

Author

Tanjib Ahmed

Roll No. 1804023

Supervised by

Dr. Md. Kamal Hosain

Professor

Department of Electronics & Telecommunication Engineering

Rajshahi University of Engineering & Technology

Heaven's Light is Our Guide

Department of Electronics & Telecommunication Engineering

Rajshahi University of Engineering & Technology, Bangladesh

CERTIFICATE

*This is to certify that the thesis paper entitled "**Numerical Study of Surface Plasmon Resonance Biosensor Employing Bismuth Ferrite, Black Phosphorus and Zinc Telluride for Blood Group Detection**" has been carried out by **Tanjib Ahmed** under the supervision of **Dr. Md. Kamal Hosain**, Professor, Department of Electronics & Telecommunication Engineering, Rajshahi University of Engineering & Technology.*

Supervisor

.....
(Dr. Md. Kamal Hosain)
Professor
Department of Electronics &
Telecommunication Engineering
RUET, Rajshahi-6204.

External Examiner

.....
(Sham Datto)
Assistant Professor
Department of Electronics &
Telecommunication Engineering
RUET, Rajshahi-6204.

Head

.....
(Dr. Fateha Samad)
Professor
Department of Electronics &
Telecommunication Engineering
RUET, Rajshahi-6204.

Declaration

I hereby declare that this submission is my own work and to the best of my knowledge and belief, it contains no material previously published or written by another person, nor material which to a substantial extent has been accepted for the award of any other degree or diploma at ETE, RUET or any other educational institution, except where due acknowledgement is made in the thesis. Any contribution made to the research by colleagues, with whom I have worked at RUET or elsewhere, during my candidature, is fully acknowledged.

I also declare that the intellectual content of this thesis is the product of my own work, except to the extent that assistance from others and is acknowledged.

Author

.....

(Tanjib Ahmed)
Roll No. 1804023
Department of Electronics & Telecommunication Engineering
Rajshahi University of Engineering & Technology
Rajshahi-6204, Bangladesh.

Abstract

An optimized prism-based surface plasmon resonance (SPR) sensor, containing a specific material combination, is represented for the accurate detection of the human blood group at a wavelength of 633nm. The sensor structure includes a BK7 prism as a substrate followed by sequential deposition of Silver (Ag), Bismuth ferrite ($BiFeO_3$), Black Phosphorus (BP), and Zinc Telluride (ZnTe). The angular interrogation method (ATM) is used for investigating the biosensor's performance parameters which include sensitivity, detection accuracy, and quality factor. The finite element method (FEM) method is used for the realization of the design and performance analysis. Optimization of the thickness of the layers is done to get the highest possible outcome. For resonance and non-resonance conditions, magnetic field propagation and electric field distribution are determined which specifies an enhanced electric field at the metallic layer. The enhanced electric field is the result of the metallic layer which reflects and redirects the electric field and gives a significant advancement in the performance parameter. The numerical calculations of the sensor are held with the sensing medium immobilized with different blood groups (A, B, O). The highest sensitivity, detection accuracy, and quality factor for the detection of blood group A are 298.17 deg/RIU, 2.2, and 130.1 RIU^{-1}; for the detection of blood group B are 327.79 deg/RIU, 1.98, and 95.35 RIU^{-1}; and for the detection of blood group C are 330.86 deg/RIU, 1.73, and 81.33 RIU^{-1} respectively. The numerical analysis of the sensor's parameters assures a significant improvement in the performance compared to previous research studies.

Keywords: Blood groups, Surface plasmon resonance, biosensor, sensitivity, transfer matrix method, black phosphorus, bismuth ferrite, zinc telluride

Acknowledgement

This report has been submitted to the Department of Electronics & Telecommunication Engineering of Rajshahi University of Engineering & Technology (RUET), Rajshahi-6204, Bangladesh. Report title regards to "**Numerical Study of Surface Plasmon Resonance Biosensor Employing Bismuth Ferrite, Black Phosphorus and Zinc Telluride for Blood Group Detection**".

First and foremost, I offer my sincere gratitude and indebtedness to my project supervisor, **Dr. Md. Kamal Hosain**, Department of Electronics & Telecommunication Engineering who has supported me throughout my project with his patience and knowledge. I shall ever remain grateful to him for his valuable guidance, advice, encouragement, cordial and amiable contribution to my project.

I wish to thank my friends who have helped me with their knowledge and experience regarding the subject matter.

Finally, I want to thank my parents for always supporting me in every field of life. Without their contribution, I would not be able to reach the place where I am today. So my unending gratitude to them.

Tanjib Ahmed

Contents

List of Figures

List of Tables

List of Symbols

S	Sensitivity
DA	Detection Accuracy
QF	Quality Factor
LOD	Limit of Detection
FWHM	Full Width Half Maxima
EFIEF	Electric Field Intensity Enhancement Factor
ϕ	Phase change at resonance angle
λ	Wavelength of the incident light
$\theta_{\mathbf{SPR}}$	SPR angle
$\nabla\theta_{\mathbf{SPR}}$	SPR angle shift
$\theta_{\mathbf{SPR}}$	SPR angle
$\mathbf{r_p}$	Reflectance Intensity
n	Refractive Index

Chapter 1

Introduction

1.1 Introduction

Blood group identification is of utmost importance in medical science. The blood types of patients must be determined before treating those who have lost a lot of blood. It is also essential that the blood groups of the patient and the donor are compatible to avoid a situation of blood incompatibility during the transfusion process [1]. For all blood transfusions, the "A," "O," and "B" blood typing systems are always examined first due to their potent specific antigen-antibody interactions. The reason for this is that any other system might be seriously harmed by the "A," "O," and "B" blood identification systems [2]. In biochemical sensing, the surface plasmon-based biosensor have been widely utilized for a few decades. Their distinguishing characteristics including dependability, label-free detection, better sensitivity, and real-time detection capability make them suitable for applications based on sensing [3, 4, 5, 6, 7]. For sensing applications, various SPR-based sensor configurations based on optical fiber, grating, prism, and coupled waveguide were developed. In most of the studies, the Kretschmann configuration-based prism-based biosensor has been examined in which a metal film is deposited on a prism basis [8]. The attenuated total reflection (ATR) phenomenon is followed by the prism-based biosensor[9]. The thin metal layer at the prism-metal interface is penetrated by evanescent waves with exponential attenuation created by the transverse magnetic (TM) polarized input wave [10]. At the interface of the metal-sensing layer, it produces surface plasmon. The resonance angle is affected by changes in the analyte's refractive index (RI)[11][12]. In the proposed work a multilayer configuration is suggested for detecting the human blood group, utilizing the immense features of BP, BiFeO3, and ZnSe. This structure with various combinations and thicknesses is theoretically studied using the TMM approach. For every structure optimization, the reflectance

curve for various angles of incidence is displayed. The performance characteristics, including angular sensitivity (S), detection accuracy (DA), fixed width at half maximum (FWHM), quality factor (QF), and limit of detection (LOD) are analysised. This research could lead to the development of a quick and precise blood group sensor.

1.2 Motivation

In the ever-evolving field of biomedicine, finding new approaches to medical diagnosis has become essential. Among these, blood group identification and analysis are of great importance, impacting a variety of fields from organ transplantation to transfusion medicine. When we explore more into various aspects of blood group identification, we find that conventional methods, although successful, can involve difficult steps and lengthy processing times. Still, there is a chance to transform this vital part of healthcare with the advent of new technologies like Surface Plasmon Resonance (SPR) sensors. A new approach in blood group identification is introduced by the integration of prism-based SPR sensors, which provide outstanding sensitivity, efficiency, and accuracy. Utilizing the principles of SPR, which allows for the real-time monitoring of changes in refractive index at the sensor surface, this technique enables rapid and label-free detection of blood groups with minimal sample requirements. These capabilities enable enhanced safety for patients and healthcare outcomes by simplifying diagnostic workflows and reducing the risk of errors associated with traditional approaches. Prism-based SPR sensors also used for a wide range of tasks, such as drug discovery and antibody-antigen interactions, in addition to blood group classification. Thus, exploring the complexities of this recently developed method in the context of blood group identification not only closes a significant gap in current diagnostic procedures but also opens the door to innovative advances with broad implications for clinical settings.

1.3 Objectives

The main objectives of this research focused on the following topics:

1. Designing and implementing a prism-based Surface Plasmon Resonance (SPR) sensor system that is specifically developed to identify and distinguish ABO blood group antigens with a high degree of sensitivity and specificity.

2. Investigating the basic ideas behind the ABO blood group system and the underlying biochemistry of antigen-antibody interactions associated with optical properties to comprehend the foundation of ABO blood group typing and detection.

3. Investigating various combinations of different materials, each having particular characteristics, to determine which one ultimately results in the optimal sensor combination.

4. Evaluating the SPR sensor technology's potential as a rapid automated, and affordable replacement for ABO blood group determination by comparing its sensitivity and specificity to well-established conventional blood typing techniques.

1.4 Research Contribution

The main research contributions are given bellow:

1. The key contribution lies in the selection of unique sensor structures, which involves careful consideration of materials possessing specific characteristics ideal for SPR activation and detection. By meticulously choosing materials with suitable properties, such as metals and dielectrics, the sensor's performance is optimized, enabling rapid and accurate detection of blood groups.

2. Additionally, the optimization of sensor parameters, including material composition and layer thickness, plays a crucial role in enhancing the sensor's sensitivity and facilitating efficient blood group identification. Thus, the main target is to propose a structure that provides optimal performance making a trade-off between the performance parameters while prioritizing the sensitivity of the sensor to have an optimal sensor.

1.5 Work Flow

The block diagram in figure 1.1 illustrates the pipeline of the research work. The primary goal of this study is to delineate the thesis objective, with a specific focus on introducing a sensor endowed with heightened sensitivity to overcome constraints identified in prior studies. This involves a thorough review of existing literature on blood group detection and optical sensor technology to pinpoint gaps and potential enhancements. Subsequently, a new sensor structure is proposed to meet the defined objectives. The optimization process entails evaluating various combinations of layer thicknesses using MATLAB to determine the configuration yielding optimal sensitivity. Following this, the chosen configuration undergoes design in COMSOL Multiphysics to simulate sensor performance. Each simulation records sensor response for different sensing elements, monitoring changes in the SPR signal. Finally, performance parameters such as sensitivity, detection accuracy, and quality factor are computed for further inspection and performance comparison with the previous works.

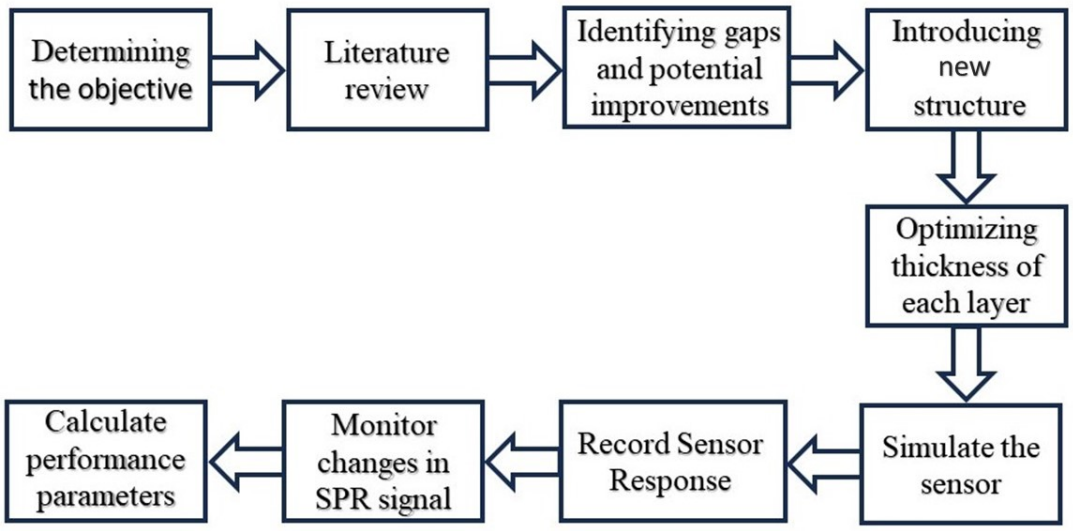

Figure 1.1: Visual representation of the research pipeline.

1.6 Thesis Outline

The research study has been organized into five chapters:

Chapter 1 includes an extensive study of prism-based surface plasmon resonance (SPR) sensors for ABO blood group detection. It outlines the motivation and goals of the thesis as well as any drawbacks in the conventional way of detection as well.

Chapter 2 provides a comprehensive review of earlier studies on human blood group detection, with an emphasis on the techniques and materials used along with the respective output parameters. The understanding regarding the limitations and advancements of the field is based on this review.

Chapter 3 conveys a detailed analysis of the theoretical foundation of the proposed blood group typing sensor. Different sensor configurations and the underlying mathematical models and material science concepts are investigated thoroughly. A comprehensive theoretical framework for the ensuing experimental work is provided in this chapter.

Chapter 4 demonstrates the sensor experiment results along with the reasoning behind the choice of particular materials, prism configurations, and thickness of each layer. The analysis is supported by relevant figures and performance metrics, culminating in a comparison with previously published works. This section offers insights into the effectiveness of the proposed sensor design.

Chapter 5, which is the final chapter of the thesis provides a comprehensive conclusion, summarizing the key findings and performance parameters of the sensor. It also explores future research directions that could be taken to improve the functionality and applicability of the sensor. This chapter serves as a culmination of the study's outcomes and sets the stage for further advancements in the field of blood group detection technology.

Overall, these chapters offer an organized framework for comprehending the development, implementation, and future advancements of prism-based SPR sensors for ABO blood group detection.

Chapter 2

Literature Overview

Blood group identification is crucial for many medical treatments, including organ transplants and blood transfusions. A person's blood type must be accurately determined in order to guarantee safe and efficient medical procedures. Many techniques and technologies have been developed over time for blood group detection; each has benefits and drawbacks of its own. Blood group detection through conventional methods involves manual tests and chemical reagents, which are prone to human error and take a considerable amount of time. Moreover, these approaches require intrusive blood collection techniques, which causes discomfort to patients. New methods have been suggested as a solution to these drawbacks. Table 2.1 represents a comprehensive literature review on sensor configurations at a wavelength of 633nm has been conducted, encompassing various methodologies, result analyses, and limitations.

Rakhshani et al. (2017) proposed a small sensor design composed of silver nanorods and metal-insulator-metal waveguides for blood group detection. Their methodology involved time-domain simulations using finite differences to evaluate performance. They reported a refractive index sensitivity of 2320 nm/RIU for Mode 1 and 1160 nm/RIU for Mode 2. However, they noted potential limitations related to fabrication imperfections, environmental variations, and shifts in sample refractive index, highlighting the importance of stability and calibration for reliable performance.

A study by Hasan et al. (2020) utilized numerical simulations and Metal-Insulator-Metal (MIM) waveguides to optimize sensitivity for blood group detection. They employed the finite element method (FEM) for sensitivity optimization and achieved a refractive index sensitivity of 1556 nm/RIU with a figure of merit (FOM) of 14.83. However, the study lacked experimental validation and noted potential limitations related to raw material constraints and fabrication issues, as well as specificity to ethanol as a sensing medium.

Sharma et al. (2010) employed spectral interrogation combined with a fiber-optic SPR sensor for blood group detection. They optimized design parameters for accurate identification and reported a limit of theoretical detection at 10^{-4} RIU. Despite achieving refractive index sensitivity for different blood groups, they highlighted potential accuracy issues related to longer sensing regions, increased fiber core diameter, and concerns regarding contamination from the Ag layer.

Tangkawsakul et al. (2016) utilized specific antibodies and waveguide structures in conjunction with LR-SPR for blood group typing. They detected changes in surface plasmons and achieved a lower detection threshold with LR-SPR compared to conventional methods. However, they emphasized the importance of accurate calibration, immobilization, and consideration of environmental factors for reliable sensitivity, acknowledging limitations related to sample preparation and environmental influences.

Rakhshani et al. (2018) employed a hexagonal array of nanoholes and simulations to assess sensitivity for blood group detection. They achieved a sensitivity of up to 3172 nm per refractive index unit. However, they acknowledged potential limitations related to fabrication constraints, environmental factors, and noise impacting sensitivity, underscoring the need for further investigation into stability and performance under realistic conditions.

The study by Jha et al. (2010) proposes the development of a biosensor chip utilizing silicon for blood group identification. Their methodology involves utilizing curve width and angular shift for performance analysis. However, it is noted that their approach may oversimplify real-world difficulties and assume perfect conditions, potentially leading to results that do not accurately reflect sample variations. Despite this limitation, the sensor demonstrates successful plasmonic resonance, achieving angular shifts ranging from 0.123° to 0.124° across blood groups, with a Full Width at Half Maximum (FWHM) between 0.073° to 0.081°, ensuring accurate detection.

Table 2.1: Configuration of the sensor layers at 633nm wavelength.

References	Methodology	Result Analysis	Limitations
[13]	Silver nanorods and metal-insulator-metal waveguides make up this small sensor design. Time domain simulations with finite differences for performance evaluation.	Fabrication imperfections, changes in environmental variations, and complex shifts in the refractive index of the sample could affect performance. Reliability depends on stability and calibration.	The sensor's refractive index sensitivity for Mode 1 is 2320 nm/RIU, and for Mode 2, it is 1160 nm/RIU.
[14]	Numerical simulations and Metal-Insulator-Metal (MIM) waveguides are used for analysis. Using the finite element method (FEM), sensitivity was optimized.	Lacks experimental validation. Performance may be impacted by raw material limitations and fabrication issues. Sensitivity is specific to ethanol as a sensing medium.	A refractive index sensitivity of 1556 nm/RIU and a figure of merit (FOM) of 14.83 are obtained with optimized structural parameters.
[15]	Uses spectral interrogation in conjunction with a fiber-optic SPR sensor and optimizes design parameters for accurate identification.	Accuracy may be impacted by longer sensing regions and increased fiber core diameter. Ag layer presence raises concerns regarding contamination.	Limit of theoretical detection: $10^{-}4$ RIU Refractive indices sensitivity at 1.3768, 1.3788, and 1.3796 RIU for blood groups A, B, and O, respectively, at their respective SPR wavelengths.
[2]	Uses particular antibodies and waveguide structures in conjunction with LR-SPR for blood group typing and the procedures follow the detection of changes in surface plasmons.	Environmental factors affect sensitivity. Accurate calibration and immobilization are required. Accuracy is impacted by sample preparation.	The lowest detection thresholds found with LR-SPR are 1.58×10^5 cells/ml for RBC-A and 3.83×10^5 cells/ml for RBC-B. This implies a higher sensitivity of the LR-SPR chip with a 3.3×10^8 cells/ml limit.
[16]	For sensitivity assessment, a hexagonal array of nanoholes and simulations are utilized.	Performance may be impacted by fabrication constraints and simplified conditions. Environmental factors and noise have an impact on sensitivity.	The sensitivity is as large as 3172 nm per refractive index unit.

References	Methodology	Result Analysis	Limitations
[17]	Develop a biosensor chip for blood group identification using silicon. uses curve width and angular shift to analyze performance.	May ignore difficulties in the real world and assume perfect circumstances. The results of the experiment might not accurately reflect sample variations.	The sensor exhibits successful plasmonic resonance, achieving angular shifts of 0.123° to 0.124° across blood groups. With an FWHM ranging from 0.073° to 0.081°, accurate detection is guaranteed.
[15]	employs glass substrates made of silica or chalcogenide for SPR sensing. assesses the accuracy of angular interrogation in blood group detection.	Accuracy is limited by the absence of blood refractive index data. Substrate selection is impacted by detector resolution. Practical difficulties in sample preparation.	Blood groups with an angular shift of 1.21° on fused silica and 0.23° on 2S2G chalcogenide substrate were identified by this sensor. Better accuracy is ensured by silica's wider curves (FWHM: 1.45°) and sharper at 2S2G (FWHM: 0.16°).
[18]	Optimizes SPR biosensor with theoretical modeling with the transfer matrix method. The sensor utilizes a Kretchmann configuration with a struncture of ().	A theoretical focus might not accurately reflect actual circumstances. Practical issues are not covered. The model's assumptions limit its applicability.	The sensor obtained a sensitivity of 0.117 deg, and a detection accuracy of 29.06 RIU^{1}.
[19]	Optimizes SPR biosensor with theoretical modeling with the transfer matrix method. The sensor utilizes Kretchmann configuration with a structure of ().	A theoretical focus might not accurately reflect actual circumstances. Practical issues are not covered. The model's assumptions limit its applicability.	The sensor obtained a sensitivity of 160 deg RIU^{1}, detection accuracy of 0.75188, and quality factor of 115.95 RIU^{1}.

Sharma et al. (2010) focus on the design considerations of surface plasmon resonance (SPR) sensors for blood group detection, employing glass substrates made of silica or chalcogenide. Their analysis assesses the accuracy of angular interrogation in blood group identification. However, the accuracy is constrained by the absence of blood refractive index data, and practical difficulties in sample preparation are acknowledged. Despite these limitations, their sensor successfully identifies blood groups with varying angular shifts on different substrates, ensuring improved accuracy with specific substrate choices.

Raghuwanshi et al. (2023) conduct a numerical study to optimize SPR biosensors using theoretical modeling with the transfer matrix method. Their sensor configuration utilizes a Kretschmann setup. While their theoretical approach might not fully capture real-world conditions and practical issues are not addressed, the sensor achieved a sensitivity of 0.117 degrees and a detection accuracy of 29.06 RIU^{-1}.

Pandey et al. (2023) also optimize SPR biosensors using theoretical modeling with the transfer matrix method, employing a Kretschmann configuration. Similar to Raghuwanshi et al., their study focuses on theoretical aspects without addressing practical issues. Nevertheless, their sensor achieves a high sensitivity of 160 degrees RIU^{-1}, a detection accuracy of 0.75188, and a quality factor of 115.95 RIU^{-1}.

Both studies with SPR sensors emphasized the importance of a buffer layer to prevent oxidation and contamination of blood samples. However, the performance parameters achieved from these biosensors can be enhanced by using different combinations of materials and optimization of the layers. As the prism-based SPR sensor gives promising results the research of the blood group detection is going with this method.

The limitations of the performance can be overcome by utilizing a multilayer configuration with optimized thicknesses of materials possessing unique characteristics. With these configurations limitations can be transcended, optimizing performance across various parameters.

Chapter 3

Fundamental Principles and Proposed Design Concept

3.1 Theoretical Background

Over the past few decades, surface plasmon-based biosensors have gained significant application in the field of biochemical sensing. They are ideal for a variety of sensing applications due to their unique characteristics, which include dependability, label-free detection, increased sensitivity, and real-time monitoring capabilities. SPR-based sensors with different topologies that use coupled waveguides, gratings, prisms, and optical fibers have been created for sensing applications. Of these, research has mostly focused on the Kretschmann configuration-based prism biosensor, which deposits a metal layer on a prism substrate [20]. Moreover, attenuated total reflection (ATR) is the basis for the operation of this prism-based biosensor [20]. Prism-based SPR sensors are based on the surface plasmon resonance principle, which describes what happens when light interacts with a metal-dielectric contact under certain circumstances. The incoming light produces a surface plasmon wave, which causes the reflectance spectrum to abruptly dip. This resonance angle shift can be measured to gather important details about the interactions taking place at the sensor surface. Remarkable advancements in the design, materials, and signal augmentation methods of the sensor have been made as a result of this effective though straightforward approach.

3.1.1 Angular Interrogation Procedure(ATR)

The angular interrogation approach using ATR has gained increasing traction among different SPR-based sensors in recent years due to its exceptional performance features, com-

mercial standardization, and simplicity of manufacturing technology. Due to a mismatch in momentum, when light is directly coupled to the metal-dielectric contact, the SPs are not sufficiently stimulated to produce SPWs [21]. Researchers have proposed a number of unique configurations, including the Otto configuration [22] and Kretschmann configuration [23, 20], which are seen in Figure 3.1, to change the photon's momentum and couple it with the SPPs, causing SPW to propagate. There is a distance in the prism-based Otto setup where a dielectric layer with a lower RI is placed between the prism and the metal sheet where the light is used. On the other hand, with the Kretschmann configuration, the metallic layer and prism are in direct contact. In order to guarantee the coupling of the strongest evanescent wave traveling through the metal and generating SPW, the Kretschmann configuration is the most widely used option among them [24, 25, 26]. In the Kretschmann setup, a high-index prism is used to incident light at the metal-dielectric interface [27].

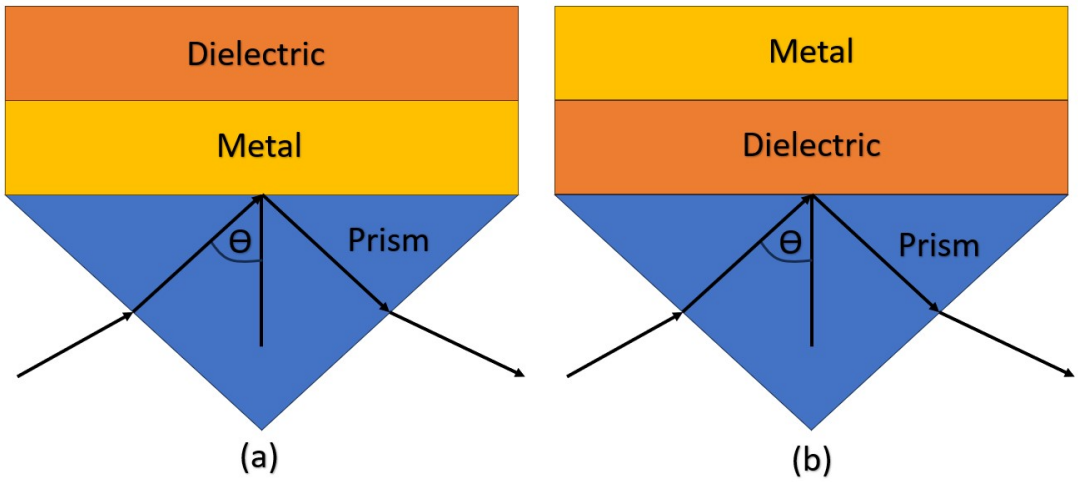

Figure 3.1: (a) Kretschmann configuration and (b) Otto configuration to match incident photon and SPW momentum.

The incident light often returns to the interface and only a little fraction passes through the metal, creating the evanescent field. The momentum of the evanescent field aligns with the SPW wave vector at a specified angle known as the resonance angle for a specific sensor arrangement and light frequency [26]. At this resonance condition, maximum light is coupled to the oscillating electrons, resulting in the least reflection. A resonance dip in the reflection spectrum referred to as an SPR point, which is extremely responsive to the RI of

the sensing medium, can be observed if the reflected light is plotted in relation to the incident angle. This SPR point can be interrogated to quickly identify the analyte.

3.1.2 Multilayer Configuration

Conventional SPR-based sensors suffer from some limitations in maximizing performance when analyzing small analyte quantities [28]. These limitations have led researchers to investigate ways to develop multilayer SPR sensors, which greatly improve sensor performance by combining several 2D nanomaterials, perovskite materials, semiconductor materials, and plasmonic materials [29, 30, 31, 32]. The selection of a low refractive index prism is due to its capacity to yield enhanced sensitivity and superior performance [33]. Silver (Ag), copper (Cu), aluminum (Al), and gold (Au) are plasmonic metals that are notable for their high SNR ratio, exceptional sensitivity, and a noticeable sharp drop in the SPR curve [34]. Perovskite materials with some exceptional features including a high dielectric constant, ferroelectricity, and piezoelectricity are barium titanate (BaTiO3), bismuth ferrite (BiFeO3), potassium niobate (KNbO3), and lead titanate (PbTiO3) [34, 35, 36]. Biosensors can benefit from materials with a high dielectric constant [37]. Moreover, due to their special qualities, two-dimensional (2D) materials including black phosphorus, graphene, and TMDs have drawn attention to SPR prism biosensors. Its tunable bandgap and high carrier mobility make it suitable for sensing applications. These materials improve sensitivity in a prism biosensor by increasing effective light-matter interactions at the sensor's surface. Since, 2D materials are thin and atomically layered, precise control over molecular interactions is possible, leading to highly selective biomolecule detection [38, 39, 40]. Because of their high refractive index and chemical stability, semiconductor materials like zinc sulfide (ZnS), zinc oxide (ZnO), and zinc telluride (ZnTe) provide a strong SPR effect [9, 41].

3.1.3 Material Selection

The main parts and materials necessary to build the sensor setup are listed in the materials section of a prism-based Surface Plasmon Resonance (SPR) sensor. The metal film, prism, and any other materials necessary for the sensor's operation are normally described

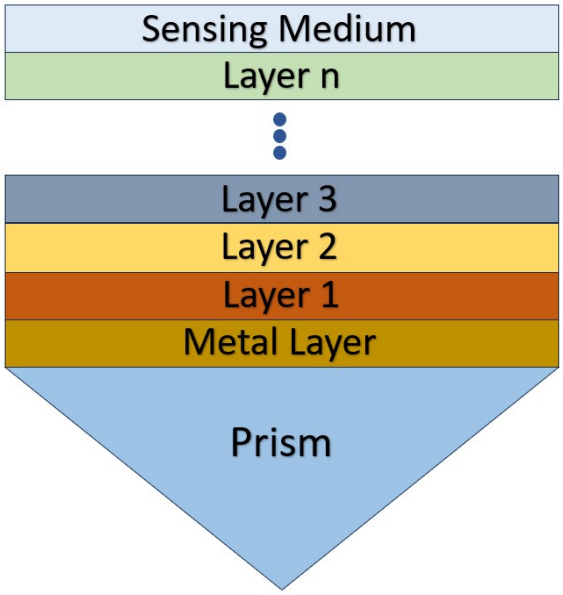

Figure 3.2: Multilayer configuration of prism based SPR sensor.

in depth. Here, as SPR active metal Au, Ag, Al, Cl, etc. materials are used for the sensing purpose of the sensor. As the electrons on the surface of the metal directly involve the operation of the sensor. Al and Cu have not attracted much interest for application because of their high-damping nature, tendency for oxidation and corrosion, and interband transition characteristics. However, Silver (Ag) can be suggested as a promising choice for SPR sensors due to its exceptional optical characteristics, which include a stronger resonance peak [42, 43, 44], a lack of interband transfer at the visible light frequency, and minimal optical damping. Ag in SPR sensors enables higher sensitivity, but they have poor chemical stability because they produce rigid oxide layers when used with liquid analyte [45]. Applying a bimetallic layer to the Ag surface, according to some studies, can overcome this issue [46, 47]. Au, on the other hand, is less prone to corrosion and oxidation issues than Ag and is more chemically stable. However, gold has a wider SPR curve and slightly higher damping loss, which reduces the detection accuracy and figure of merit (FOM) of the sensors [48]. Due to the minimal biomolecular adsorption properties of the gold surface, the sensitivity of Au-based sensors is also marginally reduced. To increase the ultimate performance of the sensor, some other materials are used. The combined SPR-based sensors setup employs several 2D materials. Because of its chemical inertness and strong adsorption properties, a

single-atom thick carbon nanostructure called graphene is frequently used on top of plasmonic materials to prevent oxidation issues and improve the performance of the sensors. It also increases the total absorption of the sensor [49, 50]. On top of the metal, there can be used some other nanomaterials to increase the performance of the sensor, which concludes transition metal dichalcogenides (WS_2, WSe_2, $PtSe_2$, $SnSe_2$, TMDCs: MoS_2, $MoSe_2$, etc.), graphene oxides, graphene carbon nitrite (g-C_3N_4), transition metal chalcogenides ($TaSe_3NbSe_3$), transition metal oxides (TMOs: $LaVO_3$, $LaMnO_3$), group IV elements [51, 52], hexagonal boron nitride (hBN), black phosphorene (BP) and the rest.

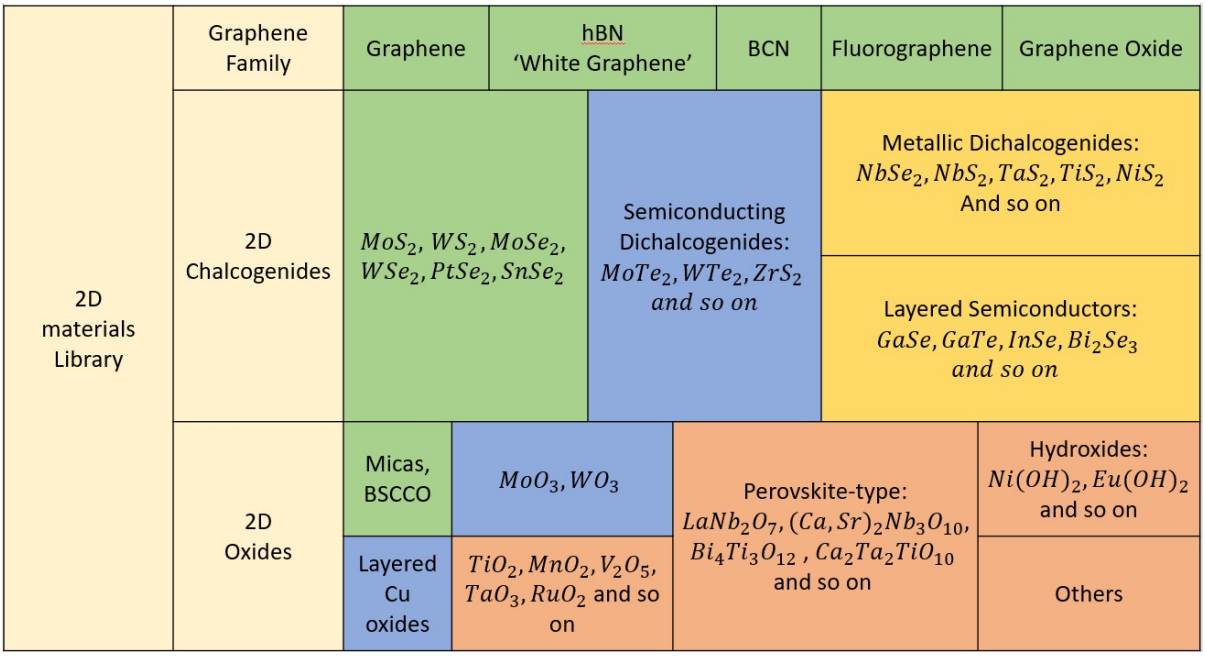

Figure 3.3: Illustration of the categorization of various material types.

3.1.4 Mathematical Modeling

Numerical analysis of the sensor is performed to determine the reflectance for a multilayer structure by the use of the transfer matrix approach and the Fresnel equation. [40]. Each layer's thickness varies in the perpendicular direction shown by the z-axis. The boundary conditions at the interfaces of the first and last layers are Z=Z_1=0 and Z=Z_{n1}, respectively. The route layer's dielectric constant is equal to the square of its refractive index. These methods use no approximation, allowing them to produce correct findings quickly. The transfer

matrix expresses a relationship between the tangential components of the first and last layers' electric and magnetic fields, and the relationship is represented as Eq. 3.1 [53]:

$$\begin{bmatrix} E_1 \\ H_1 \end{bmatrix} = P \begin{bmatrix} E_{L-1} \\ H_{L-1} \end{bmatrix} \tag{3.1}$$

E_1 and H_1 are the tangential components of electric and magnetic fields at the first layer contact. The tangential components of electric and magnetic fields at the final layer contact are represented by E_{L-1} and H_{L-1}. P is the characteristic matrix of a multilayer structure with elements P_{ij}, which is defined as [53]:

$$P = \prod_{K=2}^{N-1} P_K = \begin{bmatrix} P_{11} & P_{12} \\ P_{21} & P_{22} \end{bmatrix} \tag{3.2}$$

$$P_K = \begin{bmatrix} \cos\beta_K & \frac{-i}{q_K}\sin\beta_K \\ -i\,q_K \sin\beta_K & \cos\beta_K \end{bmatrix} \tag{3.3}$$

Here, K is an arbitrary integer, β_K is the phase thickness, and q_K denotes the refractive indices of the respective layers, as explained by,

$$\beta_K = \frac{2\pi d_K}{\lambda}\sqrt{\epsilon_k - n_p^2 \sin^2\Theta_0} \tag{3.4}$$

$$q_K = \frac{\sqrt{\epsilon_k - n_p^2 \sin^2\Theta_0}}{\epsilon_k} \tag{3.5}$$

Here, θ_0 denotes the angle of incidence, λ is the wavelength of the incident light, and n_p denotes the prism's refractive index. For p-polarized light, the reflection coefficient r is given by,

$$r = \frac{(P_{11} + P_{12}q_L)q_1 - (P_{21} + P_{22}q_L)}{(P_{11} + P_{12}q_L)q_1 + (P_{21} + P_{22}q_L)} \tag{3.6}$$

Finally, the p-polarized light reflectance intensity is represented as

$$r_p = |r|^2 \tag{3.7}$$

a. Performance Parameters

To measure the performance of the sensor, some reliable parameters need to be calculated. The performance measurement parameters, such as sensitivity, detection accuracy, FOM, and QF, should be as high as possible to avoid false positive detection [54]. The sensitivity of the sensor utilizing the angular interrogation approach is determined by the change in the SPR point or resonance angle with a change in the RI of the sensing medium. Let the

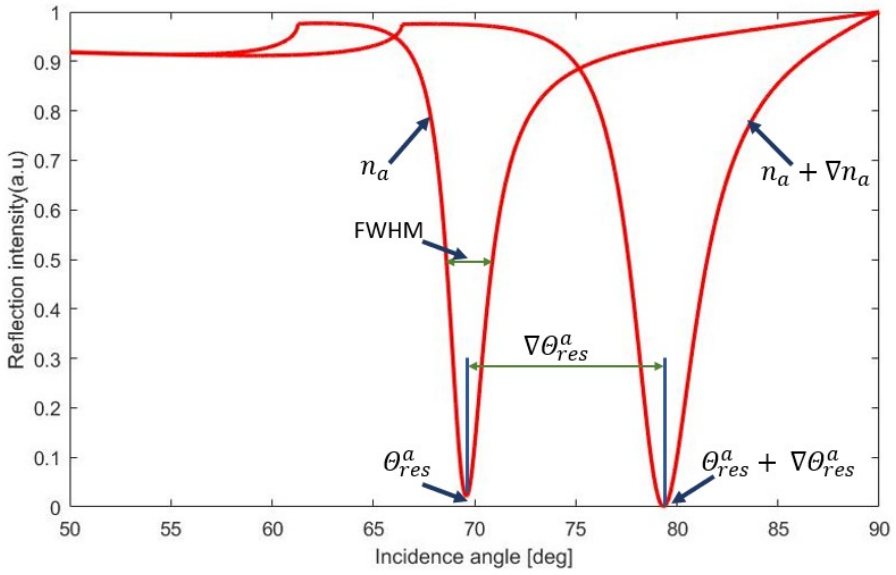

Figure 3.4: Representation of the fluctuation in the SPR curve caused by a change in the sensing medium RI.

resonance point be identified at Θ^a_{res} and $\Theta^a_{\text{res}} + \nabla\Theta^a_{\text{res}}$ for the sensing medium refractive index n_a and $n_a + \nabla n_a$, respectively as indicated in Figure 3.4. This indicates the change in the SPR curve due to the alteration in the sensing medium refractive index. The change in refractive index of n_a causes a shift in SPR, defined as $\nabla\Theta^a_{\text{res}}$. The performance parameters of the sensor are described below:

The sensitivity is defined mathematically as the ratio of change in the resonance angle (res) to the corresponding change in refractive index (n_a) [55].

$$S = \frac{\nabla\Theta^a_{res}}{\nabla n_a} \tag{3.8}$$

It is generally expressed in (°/RIU). The next SPR sensor metric is detection accuracy (DA)

or signal-to-noise ratio (SNR). It is given in terms of resonance angle change ($\nabla\Theta^{a}_{res}$) and FWHM [56].

$$DA = \frac{\nabla\Theta^{a}_{res}}{FWHM} \tag{3.9}$$

Here, FWHM defines full width at half maxima. Another essential parameter of an SPR sensor is the quality factor (QF), which may be expressed in terms of sensitivity (S) and FWHM as follows [57]:

$$QF = \frac{S}{FWHM} \tag{3.10}$$

It is commonly represented in (RIU^{-1}) units. Additionally, another critical performance metric, the limit of detection (LOD), is the quantitative measurement of the amount of biomolecules or analytes in the sensing medium and is defined as [58]:

$$LOD = \frac{\Delta n_a}{\Delta\Theta_{res}} \times 0.0573^{o} \tag{3.11}$$

LOD is computed for extremely slight shifts in the sensing medium; in this case, 0.0573° is used. Furthermore, the following expression can be used to compute the electric field intensity enhancement factor (EFIEF), which is the ratio of the square electric field at the last interface to the first layer interface [53]:

$$EFIEF = \left|\frac{E\left(\frac{L}{L-1}\right)}{E\left(\frac{1}{2}\right)}\right|^2 = \frac{\varepsilon_1}{\varepsilon_2}\left|\frac{H\left(\frac{L}{L-1}\right)}{H\left(\frac{1}{2}\right)}\right|^2 = \frac{\varepsilon_1}{\varepsilon_2}|t|^2 \tag{3.12}$$

where t is the transmission coefficient and, ε_1 and ε_L are the respective dielectric constants. Additionally, the following expression can be used to determine the phase change at resonance angle [40]:

$$\Phi = arg\,(r) \tag{3.13}$$

3.2 The Design and Modeling of the Proposed Sensor

The proposed SPR biosensor for the rapid identification of the human blood group is illustrated in 3.5. This is based on the Kretschmann configuration which consists of BK7, Ag, $BiFeO_3$, BP, and ZnTe. The BK-7 prism is used to improve detection accuracy, quality, and

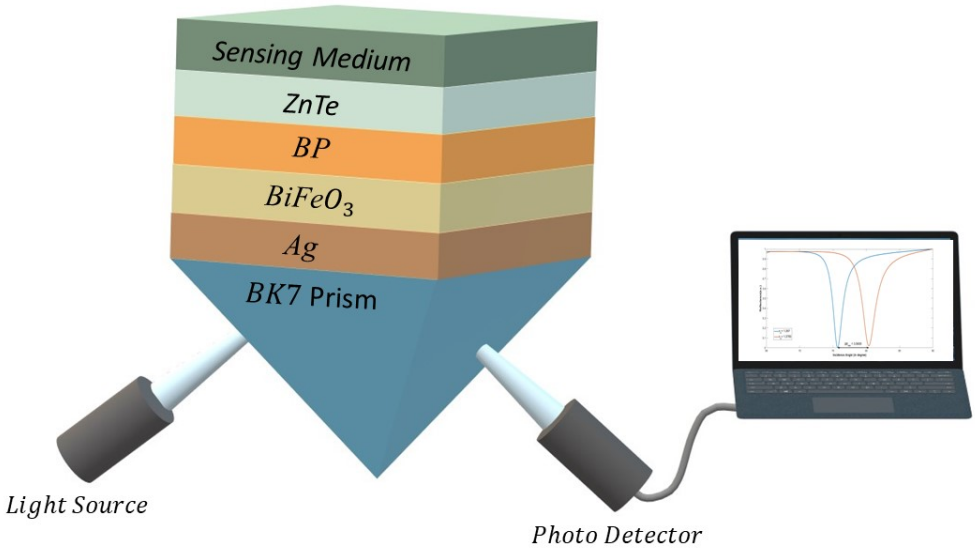

Figure 3.5: Schematic illustration of the proposed sensor.

sensitivity. The refractive index of the BK7 prism can be derived from the Sellmeier equation [59]:

$$n_{BK7}^2 = \left(1 + \frac{1.03961212 \times \lambda^2}{\lambda^2 - 0.00600069867} + \frac{0.231792344 \times \lambda^2}{\lambda^2 - 0.0200179144} + \frac{1.001046945 \times \lambda^2}{\lambda^2 - 103.560653}\right) \tag{3.14}$$

Here, λ indicates the incident electromagnetic wave wavelength.

In this configuration, silver(Ag), bismuth ferrite($BiFeO_3$), black phosphorus(BP) and zinc telluride(ZnTe) layers are used.

A silver(Ag) layer of 55nm thickness coated over a coupling prism BK-7. Because of its greater SPR ratio, Ag exhibits better sensitivity as a substrate layer. Silver's lower plasma frequency makes SPR achievable at longer wavelengths, increasing its versatility for sensing a wider range of biomolecular interactions and analyte concentrations[60]. The refractive index of the silver layer can be derived from the Lorentz-Drude model [61]:

$$n_{Ag}^2 = \left(1 - \frac{\lambda_{cw} \times \lambda^2}{\lambda_{pw}^2(\lambda_c + i\lambda)}\right) \tag{3.15}$$

In addition, bismuth ferrite ($BiFeO_3$) layer of 0.5nm thickness is deposited over the silver layer. Due to its potent piezoelectric and ferroelectric properties, the sensor layer's refractive

index is precisely controlled, resulting in increased SPR detection sensitivity. The broad bandgap of $BiFeO_3$ reduces optical losses as well, enhancing the signal-to-noise ratio of the sensor [62]. The refractive index of this material at 633nm wavelength is 2.9680 [62].

Although employing Ag as a metal in SPR sensor-based designs presents an oxidation problem, the issue is resolved by using 2D material. Thus, depositing a BP layer can solve the oxidation problem as it is a 2D material, and with its exceptional electrical qualities, high sensitivity, adjustable bandgap, and increased bio-molecule absorption, the sensor is improved by enabling precise control and higher detection [62]. The refractive index of this material at 633nm of wavelength is 3.5+0.01i [62].

Furthermore, ZnTe is deposited on top of the BP layer with a thickness of 5nm, as it has a higher refractive index and outstanding chemical stability which enables it to give a strong SPR effect [63]. Equation 3.16 gives the refractive index of ZnTe [64][65]:

$$n^2_{ZnTe} = 9.921 + \frac{0.42530}{\lambda^2 - 0.37766^2} + \frac{2.63580}{\frac{\lambda^2}{(56.5)^2} - 1} \tag{3.16}$$

Moreover, a sample of blood is drawn as the sensing medium. Based on the experimental findings for the dispersion or refractive index relation of three blood samples, the refractive index of the blood groups are indicated by the following Cauchy formula[66]:

$$n_s(\lambda)|_i = 1.357 + \frac{K_1}{\lambda^2} + \frac{K_2}{\lambda^4} \tag{3.17}$$

Here, the wavelength of the incident wave λ is at nm, and K_1 and K_2 are the Cauchy coefficients. The subscripts i in equation (3.17) refer to $i = O$, $i = B$, and $i = A$, indicating the blood samples "O," "B," and "A," respectively. Different blood types have different refractive indices followed by equation 3.17, shown in Table 3.1 [66].

Table 3.1: Refractive index of the corresponding blood group at 633nm wavelength.

Sensing Medium	Refractive Index
Blood Group 'A'	1.3739
Blood Group 'O'	1.3778
Blood Group 'B'	1.3783

The optical properties of materials with layer thickness employed in the proposed biosen-

sor model are summarized in Table 3.2, where B and T are considered as the number of layers for $BiFeO_3$ and BP. Optimization of the number of layers is utilized to get high performance.

Table 3.2: Configuration of the sensor layers at 633nm wavelength.

Materials	Refractive Index	Thickness	References
Prism(BK7)	1.5151	-	[59]
Silver(Ag)	0.056206 + 4.2776∗i	65nm	[61]
BFO($BiFeo_3$)	2.9680	B∗0.5nm	[62]
Black Phosphorus(BP)	3.5+0.01∗i	T∗0.5nm	[62]
Zinc Telluride(ZnTe)	2.9887	3nm	[64]

Chapter 4

Performance Analysis

4.1 Computational Environment and Result Generation

COMSOL multiphysics simulation software is used for the design and analysis of the suggested biosensor. The 2D geometry of the biosensor (BK7/Ag/$BiFeO_3$/BP/ZnTe/SM) is shown in Figure 4.1a. The user-controlled mesh, where each element size is set at 'Extra Fine', is depicted in Figure 4.1b. When directing light toward the top of the SF10 glass prism, pe-

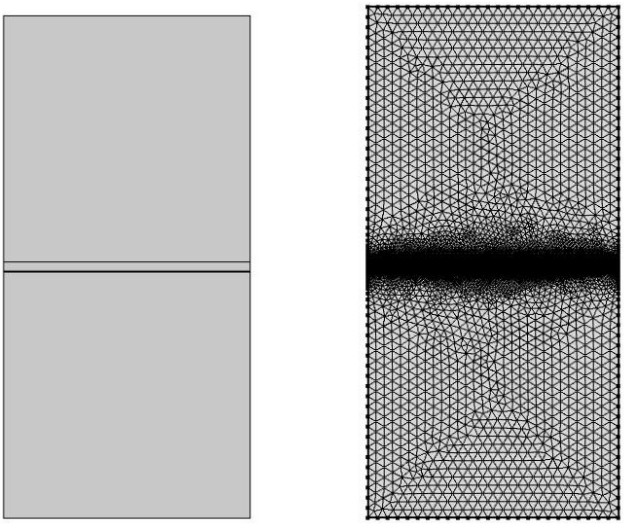

(a) (b)

Figure 4.1: Structural overview of proposed SPR biosensor: (a) 2D structural overview (b) Mesh analysis.

riodic ports in the frequency domain and Foquet periodicity in a periodic condition are selected in the context of electromagnetic waves. The simulation of the SPR biosensor is performed using a frequency domain solver with a frequency of $3 \times 10^8/\lambda$ Hz. For incident angles, a parametric sweep with 0.0573-degree increments is utilized, encompassing an angle range of 65 degrees to 90 degrees by angular interrogation. The output reflectance

intensity curve is used to calculate the resonance angle. By simulating the variations in output reflectance intensity, sensor performance, and sensitivity can be calculated for every refractive index change. Both resonance and non-resonance circumstances are examined in the SPR biosensor inquiry. The magnetic field propagation and electric field intensity are shown in Figure 4.2.

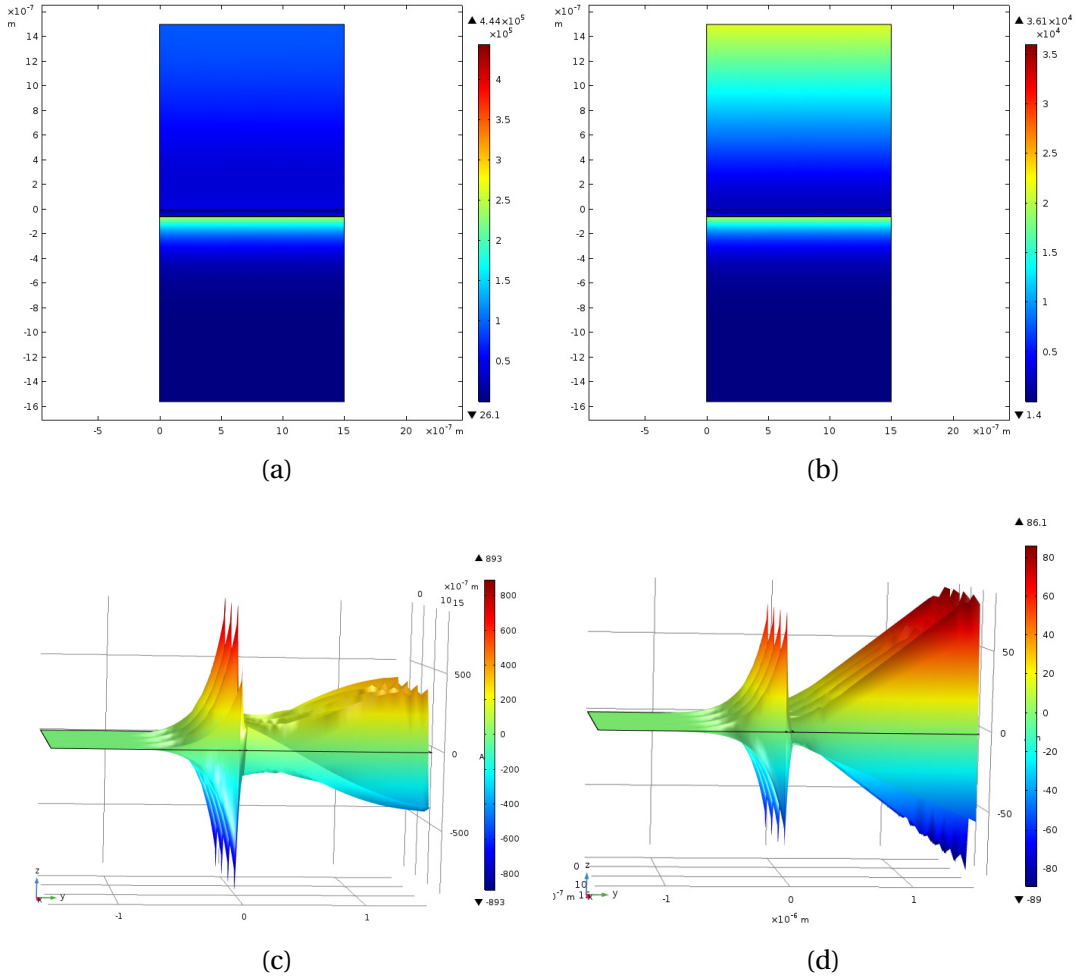

(a) (b)

(c) (d)

Figure 4.2: Norm distribution for the electric and magnetic fields: (a) An enhanced electric field with an angle(resonance) of 85.4 degrees (b) An enhanced electric field with an angle(non-resonance) of 89.6 degrees (c) An enhanced magnetic field with an angle(resonance) of 85.4 degrees (d) An enhanced magnetic field with an angle(non-resonance) of 89.6 degrees.

In the plasmonic layer, significant excitation of surface plasmons and increased localization lead to elevated electric and magnetic field intensities [67]. Electric field intensities for resonance and non-resonance circumstances are shown in Figures 4.2a and 4.2b, which

indicate that the electric field intensity passes through the metal layer only in the resonance condition. For magnetic field intensities, at a resonance angle, a substantial excitation in the plasmonic layer is detected. There is no excitation for the non-resonance angle, as seen in Figures 4.2c and 4.2d.

4.2 Result Analysis

In this study, SPR biosensor is designed based on the Kretschmann configuration, which includes a prism to give surface plasmons the necessary momentum. Due to the BK-7 prism's low refractive index, it is chosen. By using p-polarized light with a wavelength of 633 nm, surface plasmons (SP) can be coupled at the metal-dielectric interface, as shown in Figure 3.5. This work focuses on reflectance changes, due to the changes in the sensing medium. The reflectance curve (SPR curve) experiences a noticeable, pronounced dip when resonance is reached. This means that the surface plasmons receive the most energy when resonance conditions are present.

4.2.1 Selection of Silver(Ag) Layer's Thickness

It is essential to precisely control the thickness of the metallic layer to achieve the highest excitation of SPs, ideally with reflectance as close to zero as possible. The silver layer on the BK-7 prism is optimized, as indicated in Figure 4.3. A minimal reflectance of 0.0012 at the resonance angle is seen when the silver layer is 55nm thick. This is explained by a decreased energy loss during the transfer of light from the incident light to the SPs. Notably, the reflectance of the silver layer has a small Full Width at Half Maximum (FWHM), which improves the accuracy of detection. The minimal FWHM of 1.335 is achieved with a silver layer thickness of 65 nm. Therefore, a trade-off between reflectance and FWHM led to the selection of a 55 nm thickness for the silver layer, yielding reflectance and FWHM values of 0.0012 and 1.78, respectively. Besides, silver only offers a limited amount of chemical stability due to its susceptibility to oxidation. To overcome this oxidation problem, Black Phosphorus (BP), which is a 2D material, can be considered and it also improves the performance by increasing the absorption quality, since it has tunable bandgap. The BP layer

also includes other distinct characteristics, such as exact alignment on the metal coating and other special qualities like an expanded surface area and a high charge carrier density. $BeFeO_3$ and ZnTe also improve the performance parameter by increasing the absorption capability of the sensor and also have good chemical stability.

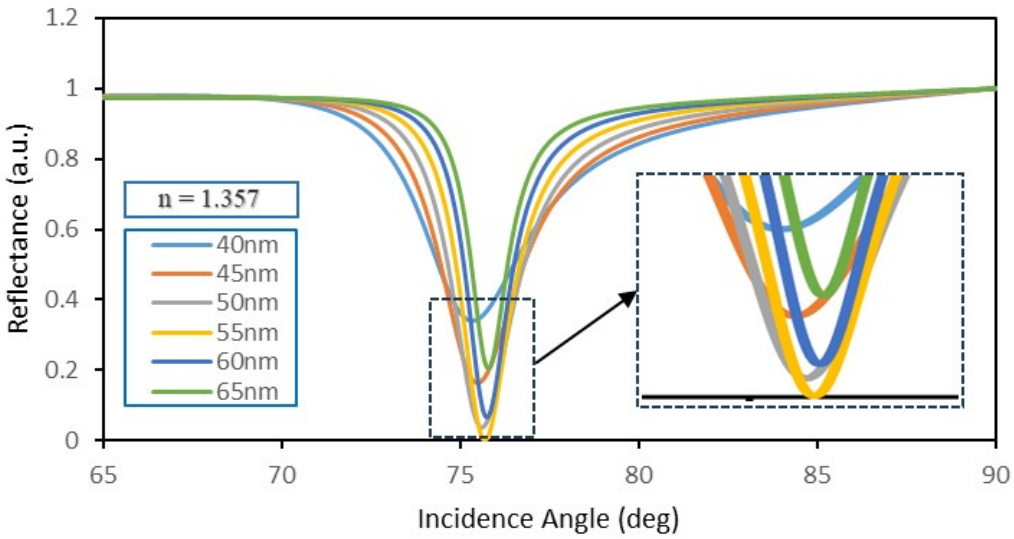

Figure 4.3: Variation in reflectance for a range of silver(Ag) thicknesses with respect to the incident angle.

4.2.2 Selection of the Optimal SPR Structure

Different forms of SPR biosensor structures are presented in table 4.1 and evaluated in this section. Figure 4.4 depicts the SPR curve for four distinct configurations applied to the prism. In Figure 4.4a, Structure I includes a two-layer setup with Ag and BP with a thick-

Table 4.1: Different Structures of SPR Structure

Serial no.	Structures	Design Configurations
1	Structure I	BK-7 Prism/Ag/BP
2	Structure II	BK-7 prism/Ag/$BiFeO_3$/BP
3	Structure III	BK-7 prism/Ag/BP/ZnTe
4	Structure IV	BK-7 prism/Ag/$BiFeO_3$/BP/ZnTe

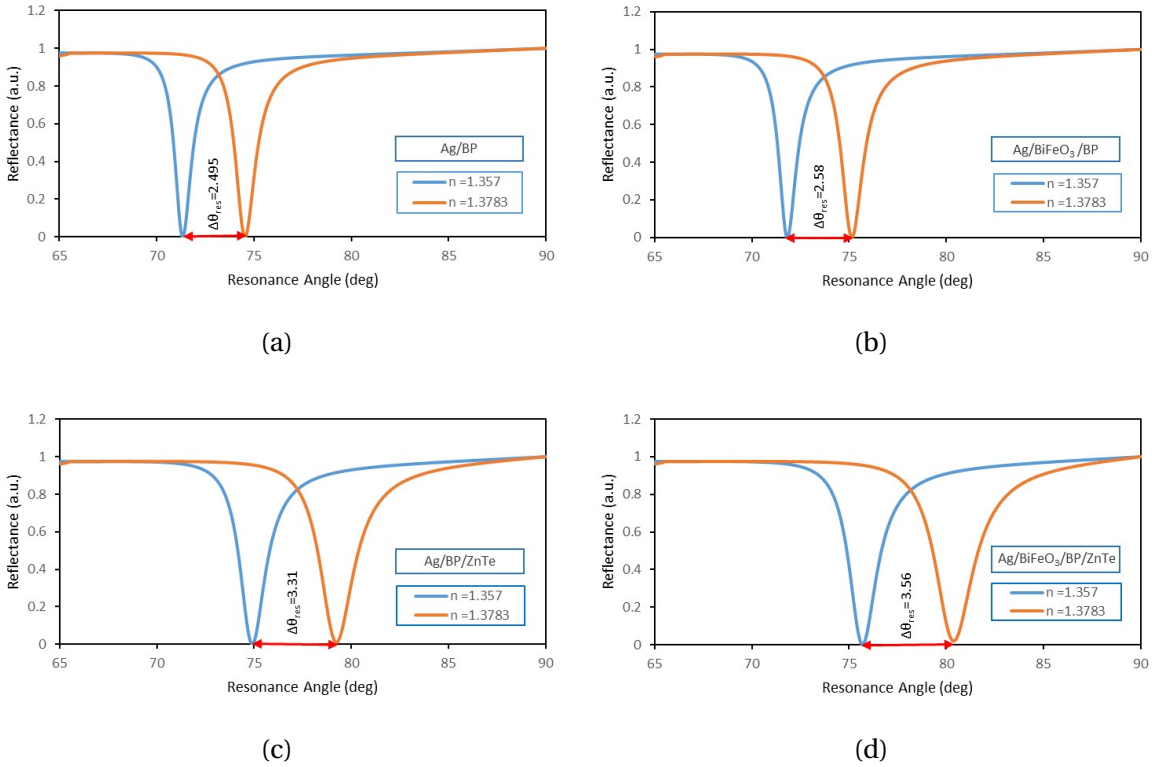

Figure 4.4: Variation of reflectance with respect to incident angle for different SPR configuration: (a) Structure I ; $\Delta\theta_{res} = 2.495$ (b) Structure II; $\Delta\theta_{res} = 2.58$ (c) Structure III; $\Delta\theta_{res} = 3.31$ (d) Structure IV; $\Delta\theta_{res} = 3.56$.

ness of 55 nm and 0.5 nm respectively, is utilized and exhibits an SPR angle change of 2.495 degrees with a corresponding sensitivity of 150.4695 deg/RIU. BP, a 2D material, is used in SPR sensor designs for solving Ag oxidation problems. This improves sensor performance by providing enhanced control, sensitivity, adjustable bandgap, and increased absorption of biomolecules.In structure II, the addition of the $BiFeO_3$ layer (with a thickness of 0.5 nm) along with Ag and BP layers modified the conventional configuration, as illustrated in Figure 4.4b. In this case, the configuration presents an SPR angle change of 2.58 degrees, and a sensitivity of 155.8685 deg/RIU is obtained. $BiFeO_3$'s strong ferroelectric and piezoelectric characteristics allow for precise adjustment of the sensor layer's refractive index, which boosts the sensitivity of SPR detection and its wide bandgap lowers optical losses as well, improving the sensor's signal-to-noise ratio. The third scenario which is depicted in Figure 4.4c, involves the configuration of structure III, integrating Ag, BP, and ZnTe layers with

thicknesses of 55 nm, 0.5 nm, and 3 nm respectively, resulting in an SPR angle change of 2.58 degrees and a sensitivity of 203.2864 deg/RIU. The addition of the ZnTe layer gives distinct chemical stability and increased refractive index allowing it to produce a powerful SPR effect. Finally, for Structure IV, incorporating Ag, $BiFeO_3$, BP, and ZnTe layers, figure 4.4d demonstrates an SPR angle change of 3.56 degrees and a sensitivity of 220.1878 deg/RIU. Hence, Structure IV out of the four structures exhibits the highest sensitivity of 220.1878 deg/RIU. However, The maximum detection accuracy and quality factor of 2.53 and 139.85 RIU^{-1} respectively, are achieved with structure I. A demonstration of each parameter for different blood groups is shown in figure 4.5. A trade-off between detection accuracy, quality

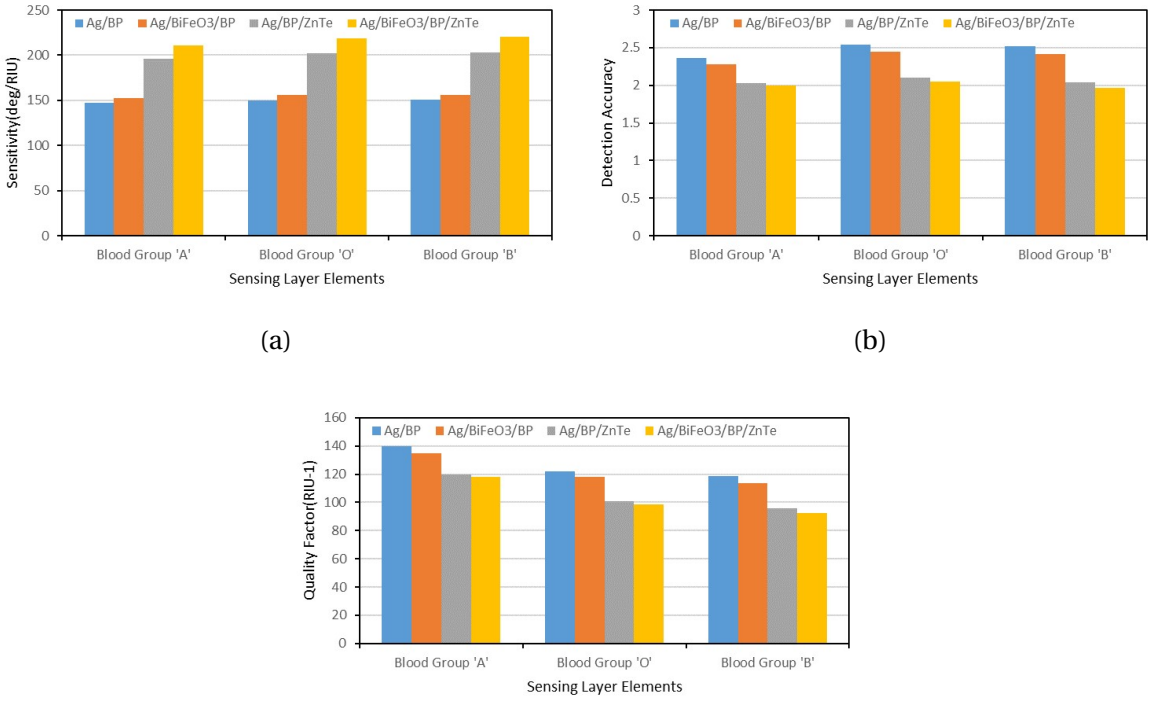

Figure 4.5: Variation of (a) sensitivity (b) detection accuracy (c) quality factor for different combinations of layers in the SPR sensor.

factor, and sensitivity led to the selection of the structure IV as the optimal choice for SPR structure, prioritizing the sensitivity of the biosensor. The selected structure yields sensitivity, detection accuracy, and quality factor of 220.1878, 2.047, and 118.27^{-1} respectively. Here, figure 4.5 demonstrates each parameters for different blood groups. Additionally, the

overall highest performance overview for all structures are briefly summarized in Table 4.2.

Table 4.2: Performance parameters for different configurations of the biosensor.

Configurations	S(^{o}/RIU)	DA	QF(RIU^{-1})
Structure I	150.4695	2.5366	139.8539
Structure II	155.8685	2.4508	135.0199
Structure III	203.2864	2.0973	119.72
Structure IV	220.1878	2.0472	118.2732

4.2.3 Effect of the Number of BFO and BP Layer

The enhancement of sensitivity and overall performance of the proposed SPR biosensor is intricately linked to the thickness and number of layers of $BiFeO_3$ and BP. Within the sensor configuration, the variation in the number of layers ranges from 1 to 4 for either $BiFeO_3$ or BP, while the other remains fixed at 1 layer. Here, the thickness of each layer of the $BiFeO_3$ and BP are taken as 0.5 nm and 0.5 nm respectively. Moreover, B and T are taken as the number of layers of $BiFeO_3$ and BP respectively. The graphical representation in Figure 4.6a illustrates the Sensitivity (S) variation for the two configurations. A clear positive correlation is observed for the configuration with the increasing number of $BiFeO_3$ layers (T =1 and B = 1 to 4). The level of sensitivity grows linearly from a baseline of 220.5753 deg/RIU (B = 1) to a peak of 330.863 deg/RIU (B = 4), highlighting the impact of additional $BiFeO_3$ layers on sensitivity enhancement. On the contrary, a more significant positive correlation is noted when sensitivity is evaluated for the configuration with the increasing number of BP layers (B = 1 and T = 1 to 4). Sensitivity gradually increases from 220.5753 deg/RIU (T = 1) to 360.4523 deg/RIU (T = 4), indicating a notable improvement associated with a higher number of BP layers. Based on a quality factor (QF) analysis of all the configurations shown in Figure 4.6b, the configuration with increment in the $BiFeO_3$ layers (T =1 and B = 1 to 4) almost exhibits a continuous increase, rising from 132.7505 RIU$^-$1 (B = 1) to 144.3662 RIU$^-$1 (B = 4). Conversely, after going through an increasing manner from 333 to 444, a slight drop in QF is observed in the arrangement with respect to the increment of BP layers (T =1 and B = 1 to 4). This decrease is observed from 132.7505 RIU$^-$1 (T = 1) to 128.3894 RIU$^-$1 (T

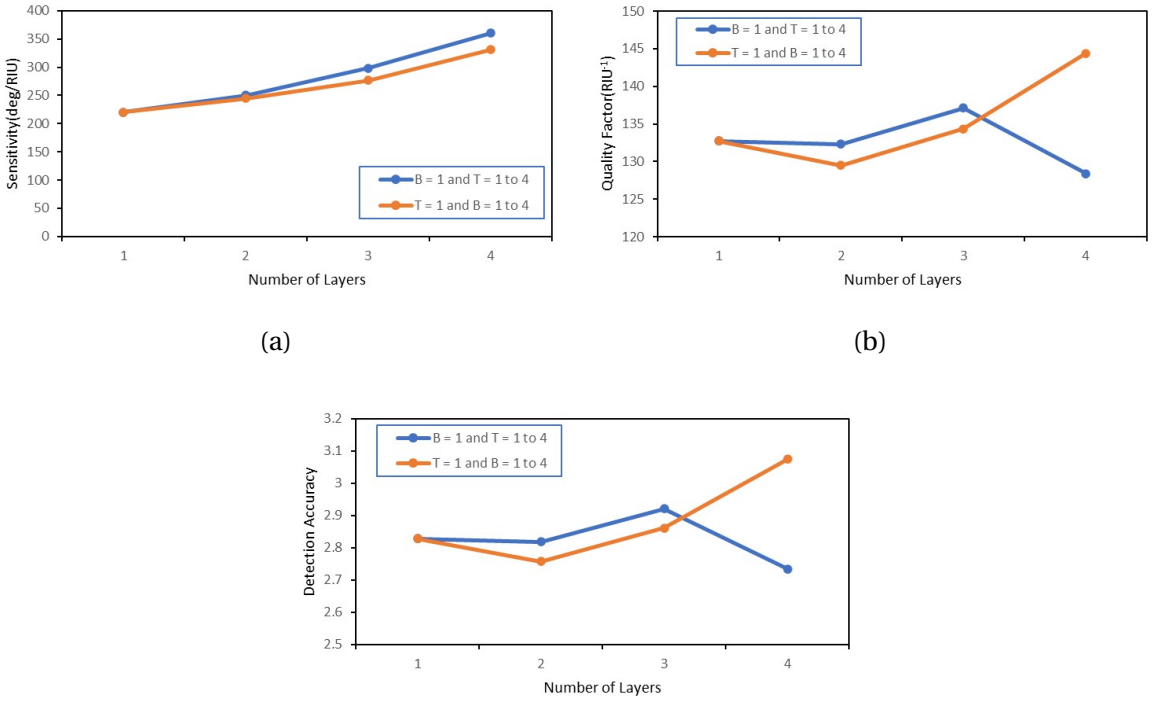

Figure 4.6: (a) Sensitivity concerning various BP and $BiFeO_3$ layer thickness combinations (b) Detection accuracy concerning various BP and $BiFeO_3$ layer thickness combinations (c) Quality factor concerning various BP and $BiFeO_3$ layer thickness combinations.

= 4). These results suggest that although different BP layers have more complex impacts, additional $BiFeO_3$ layers positively influence QF. Slight variations exist between both configurations for the detection accuracy (DA), as seen in Figure 4.6c. DA ranges from 2.8276 (B = 1) to 3.075 (B = 4) in the $BiFeO_3$ layer variation scenario (B). Similarly, DA fluctuates very little in the context of BP layer variation (T), falling between 2.8276 (T = 1) and 2.7347 (T = 4). These results suggest that by changing either the $BiFeO_3$ or the BP layers, the detection accuracy varies with respect to the increasing number of layers in a similar manner to that of the quality factor. However, the highest achieved QF and DA are 144.3662 $RIU^{-}1$ and 3.075 respectively for the number of $BiFeO_3$ layer as 3 and BP layer as 1. Therefore, a trade-off between detection accuracy, quality factor, and sensitivity led to the selection of the combination as the optimal choice for SPR structure, where the number of the BiFeO3 layers is there and the BP layer is one. Thus, the final configuration has detection accuracy, quality

factor, and sensitivity of 144.3662 RIU$^-$1, 3.075, and 330.863 RIU$^-$1 respectively. Table 4.3 demonstrates the performance parameters of this optimized sensor.

Table 4.3: Performance parameters of the proposed biosensor for blood group detection.

Blood Group	θ_{SPR} (deg)	$\Delta\theta_{SPR}$ (deg)	FWHM (deg)	S (deg RIU^{-1})	DA	QF (RIU^{-1})	LOD
A	83.6594	5.042	3.4377	298.1668	2.2	130.1016	1.922×10^{-4}
O	85.4356	6.8182	4.068	327.798	1.9834	95.3539	1.748×10^{-4}
B	85.6647	7.0473	4.1826	330.8592	1.7324	81.3321	1.732×10^{-4}

4.2.4 Variation of Reflectance, Phase and EFIEF with Incident Angle for Different Blood Group

a. Variation of Reflectance

Figure 4.7 demonstrates the reflectance curve with respect to the variation of the incidence angle indicating the respective change in the resonance angle for different blood groups. For

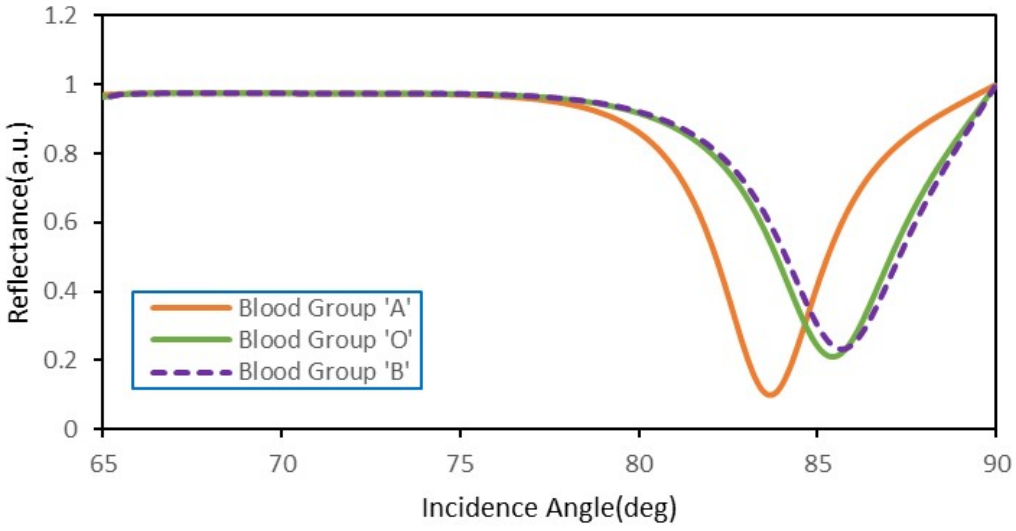

Figure 4.7: Variation of reflectance for different RI that correspond to distinct blood types.

each blood group as a sensing element, there exhibits minimal reflectivity at the resonance

angle. A reduced energy loss during the light transfer from the incident light to the SPs explains this. Notably, a respectable level of detection accuracy as shown in Table 4.3 is achieved by the minimal FWHM.

b. Variation of Phase

The phase interrogation approach, which is mathematically expressed in Eq. 3.13, has been applied to validate this structure and results. Figure 4.8 depicted the phase change vs. angle of incidence for the suggested final structure, i.e., (BK7/Ag/$BiFeO_3$/BP/ZnTe/SM). It has been found that there is a sudden phase change for the varied values of the refractive index of the sensing medium at the same corresponding resonance angle, suggesting different blood groups (A = 1.3739, O = 1.3778, and B = 1.3783). As the refractive index rises, the position of the associated phase change is observed and it shift toward the higher incidence angle side, suggesting a new blood group. This shift is caused by the structure's surface plasmon damping.

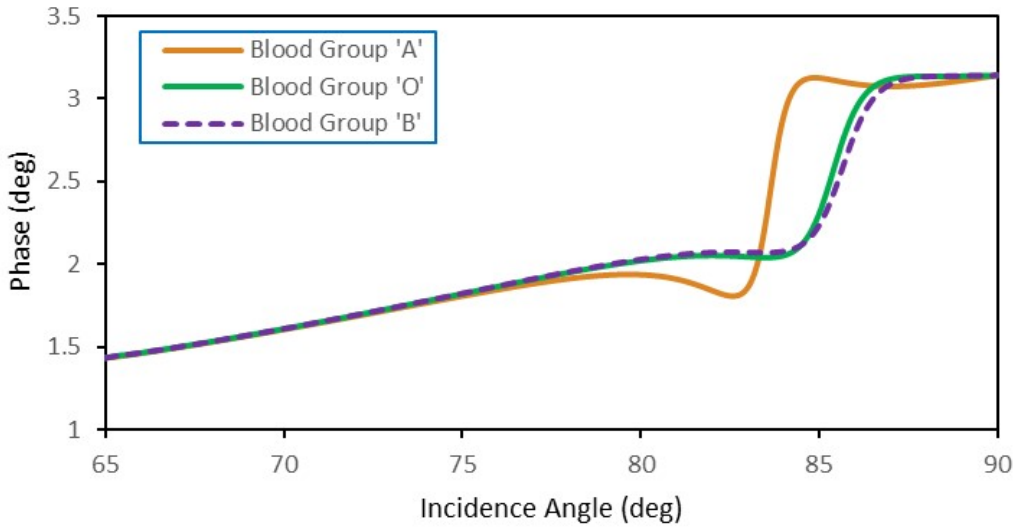

Figure 4.8: Variation of phase for different RI that correspond to distinct blood types.

c. Variation of EFIEF

An analysis of the relationship between the final structure's electric field intensity enhancement factor (EFIEF) and changes in the refractive index, which indicates various blood groups, is conducted. One important performance metric of the SPR-based biosensor is the EFIEF, which can be computed analytically using Eq. 3.12. Unlike the metal–dielectric interface, the EFIEF specifies how well the electric field can be confined in the SM. Figure 4.9 shows the matching field peak height at resonance angles for the final construction. Hence, this demonstrates that the surface plasmons are excited at resonance angle when most incident light energy is transmitted to them. Furthermore, it is noted that a drop in EFIEF occurs for each blood type which corresponds with an increase in the analyte's refractive index. This occurs mainly as a result of the analyte's gradually stronger absorption of the incident light energy.

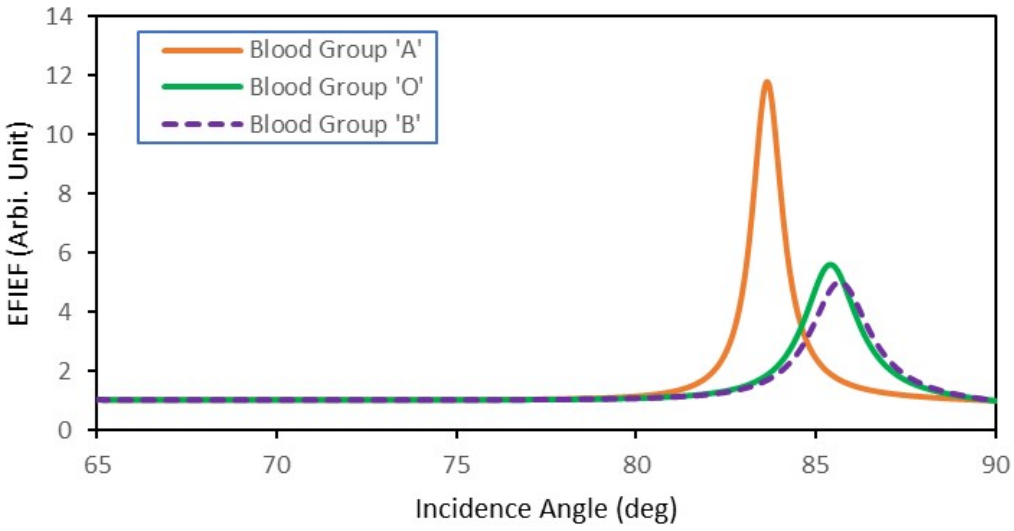

Figure 4.9: Variation of EFIEF for different RI that correspond to distinct blood types.

4.2.5 Electric Field Intensity Analysis

The complex interaction between plasmonic waves and the analyte is illustrated by Figure 4.10. Analyte interaction is greatly enhanced by these waves, possessing the unique capacity

to increase engagement even with slight variations in the refractive index. Furthermore, Figure 4.10 explicitly illustrates that the suggested configuration achieves a notable maximum field intensity of 2.32 × 105 V/m. This highlights the potential of the proposed arrangement for enhanced analytical sensitivity and performance by demonstrating its capacity to produce a strong and concentrated field.

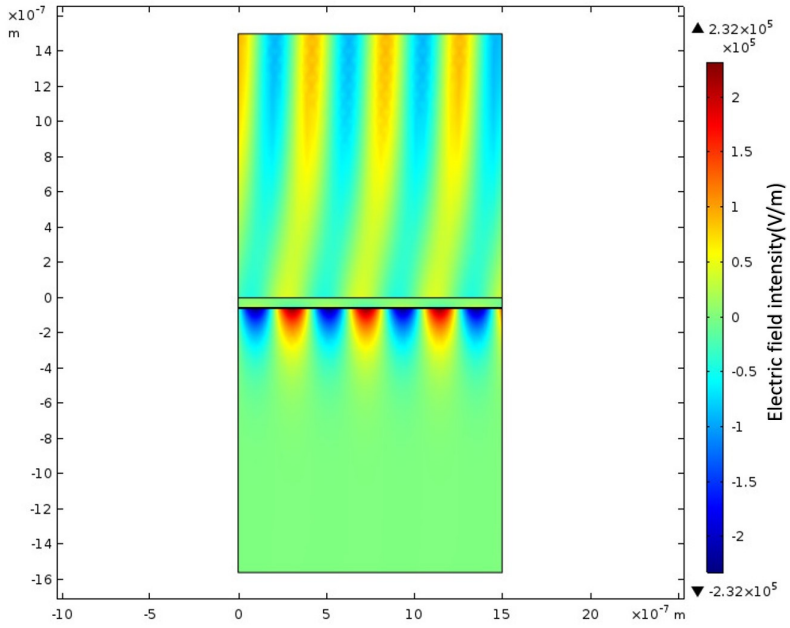

Figure 4.10: Inspection of the electric field's intensity for the surface plasmon wave.

4.3 Discussion

The comparative analysis shown in Table 4.4 illustrates the extent to which the proposed SPR biosensor performs in comparison with the recently published biosensor models. Here, the suggested biosensor exhibits sensitivity of 298.16 deg/RIU, 327.798 deg/RIU, and 330.859 deg/RIU for blood group elements 'A', 'O', and 'B', respectively. Moreover, its detection accuracies are 2.2, 1.98, and 1.73 for blood group elements 'A', 'O', and 'B', respectively. In contrast, the sensor designed by Pandey et al., provides a sensitivity of 160 deg/RIU, a detection accuracy of 0.75, and a quality factor of 115.95 RIU^{-1}, which is the most recent works in spr sensor for blood group detection [68]. And the work in [69] yields results that also fall behind that of the proposed work. As a result, compared to the previously developed blood

group sensor described in the literature, the suggested biosensor offers better performance parameters.

Table 4.4: Comparative summery between current work and earlier works.

References	Sensor Configuration	S	DA	QF
[69]	Si/Al	0.117 deg	29.06 deg^{-1}	-
[68]	BK7/Ag/Cr/HfO_2	160 deg RIU^{-1}	0.75188	115.95 RIU^{-1}
Current work	BK7/Ag/$BiFeO_3$/BP/ZnTe	330.86 deg RIU^{-1}	2.2	130.1016 RIU^{-1}

Chapter 5

Conclusions

5.1 Conclusions

SPR biosensors are widely used for biomolecule detection because of their beneficial qualities, which include fast sensing speeds, short response times, and label-free detection. Using a multilayer angular interrogation technique, this work presents the design and analysis of an SPR biosensor for the detection of human blood types In the proposed structure, the impact of the BP and the ZnTe layers and precise optimization of the thickness of the layers contributes to the high performance. The sensor provides sensitivities of 298.17 deg/RIU, 327.79 deg/RIU, and 330.85 deg/RIU for blood group samples 'A', 'B', and 'O', which are superior to the previous works. Furthermore, the detection accuracy of 2.2, 1.98, and 1.73 for blood group samples 'A', 'B', and 'O' respectively, demonstrates its precise detection and reliability. With the ability of rapid identification of blood group samples 'A', 'O', and 'B', the proposed structure represents a significant advancement in blood type biosensing technology.

5.2 Prospects of Future Research

With a wide range of potential applications and advancements, prism-based SPR sensors for blood group detection have a promising future. Future development should focus on these specific areas:

1. Enhanced Sensitivity: Further research and development attempts will focus on increasing the sensitivity of prism-based SPR sensors to a greater extent. Advanced sensor designs, novel materials, and nanostructured surfaces will be explored for this instance.

2. Multiplexing and High-Throughput Inspection: With the introduction of new multi-channel and multiplexed SPR sensors, it will be feasible to detect multiple analytes at once, reducing the time and sample requirements for experiments. Thus, along with the detection of blood groups other diagnoses can be done.

3. 2D Materials and Metamaterials: Graphene, MoS2, and metamaterials with particular plasmonic characteristics are a few examples of 2D materials that can be combined to enhance the performance of SPR sensors.

4. 3. Point-of-Care Applications: To create portable, affordable, and user-friendly devices for point-of-care applications, SPR sensors can be miniaturized and integrated with microfluidic systems.

5. Biomedical Imaging Applications: Label-free, real-time imaging of biomolecular interactions at the nanoscale will be made possible by combining SPR sensors with imaging techniques like plasmonic imaging and SPR microscopy.

In conclusion, it has a bright future due to advancements in sensitivity, multiplexing capacity, mobility, and interoperability in the diagnosis process.

Bibliography

[1] D. J. Han and T. Kenmochi, "ABO Incompatibility," in *Transplantation of the Pancreas*, R. W. G. Gruessner and A. C. Gruessner, Eds. Springer International Publishing, pp. 735–754. [Online]. Available: https://doi.org/10.1007/978-3-031-20999-4_53

[2] W. Tangkawsakul, T. Srikhirin, K. Shinbo, K. Kato, F. Kaneko, and A. Baba, "Application of long-range surface plasmon resonance for ABO blood typing," vol. 2016. [Online]. Available: https://www.hindawi.com/journals/ijac/2016/1432781/abs/

[3] J. Homola, S. S. Yee, and G. Gauglitz, "Surface plasmon resonance sensors: Review," vol. 54, no. 1, pp. 3–15. [Online]. Available: https://www.sciencedirect.com/science/article/pii/S0925400598003219

[4] S. M. Borisov and O. S. Wolfbeis, "Optical Biosensors," vol. 108, no. 2, pp. 423–461. [Online]. Available: https://pubs.acs.org/doi/10.1021/cr068105t

[5] X. Fan, I. M. White, S. I. Shopova, H. Zhu, J. D. Suter, and Y. Sun, "Sensitive optical biosensors for unlabeled targets: A review," vol. 620, no. 1, pp. 8–26. [Online]. Available: https://www.sciencedirect.com/science/article/pii/S0003267008009343

[6] E. Wijaya, C. Lenaerts, S. Maricot, J. Hastanin, S. Habraken, J.-P. Vilcot, R. Boukherroub, and S. Szunerits, "Surface plasmon resonance-based biosensors: From the development of different SPR structures to novel surface functionalization strategies," vol. 15, no. 5, pp. 208–224. [Online]. Available: https://www.sciencedirect.com/science/article/pii/S1359028611000325

[7] T. Kaminski, A. Gunnarsson, and S. Geschwindner, "Harnessing the Versatility of Optical Biosensors for Target-Based Small-Molecule Drug Discovery," vol. 2, no. 1, pp. 10–15. [Online]. Available: https://pubs.acs.org/doi/10.1021/acssensors.6b00735

[8] E. Kretschmann and H. Raether, “Notizen: Radiative Decay of Non Radiative Surface Plasmons Excited by Light,” vol. 23, no. 12, pp. 2135–2136. [Online]. Available: https://www.degruyter.com/document/doi/10.1515/zna-1968-1247/html

[9] B. Karki, A. Uniyal, B. Chauhan, and A. Pal, “Sensitivity enhancement of a graphene, zinc sulfide-based surface plasmon resonance biosensor with an Ag metal configuration in the visible region,” vol. 21, no. 2, pp. 445–452. [Online]. Available: https://link.springer.com/10.1007/s10825-022-01854-4

[10] J. Sun, H. Du, Z. Chen, L. Wang, and G. Shen, “MXene quantum dot within natural 3D watermelon peel matrix for biocompatible flexible sensing platform,” vol. 15, no. 4, pp. 3653–3659. [Online]. Available: https://link.springer.com/10.1007/s12274-021-3967-x

[11] P. Bhatia and B. D. Gupta, “Surface-plasmon-resonance-based fiber-optic refractive index sensor: Sensitivity enhancement,” vol. 50, no. 14, pp. 2032–2036. [Online]. Available: https://opg.optica.org/abstract.cfm?uri=ao-50-14-2032

[12] Y. Xu, L. Wu, and L. Ang, “Surface Exciton Polaritons: A Promising Mechanism for Refractive-Index Sensing,” vol. 12, no. 2, p. 024029. [Online]. Available: https://link.aps.org/doi/10.1103/PhysRevApplied.12.024029

[13] M. R. Rakhshani and M. A. Mansouri-Birjandi, “High sensitivity plasmonic refractive index sensing and its application for human blood group identification,” vol. 249, pp. 168–176. [Online]. Available: https://www.sciencedirect.com/science/article/pii/S0925400517306652

[14] Numerical investigation of an optimized plasmonic on-chip refractive index sensor for temperature and blood group detection - ScienceDirect. [Online]. Available: https://www.sciencedirect.com/science/article/pii/S2211379720320489

[15] A. K. Sharma, R. Jha, and H. S. Pattanaik, “Design considerations for surface plasmon resonance based detection of human blood group in near infrared,” vol. 107, no. 3, p. 034701. [Online]. Available: https://doi.org/10.1063/1.3298503

[16] M. R. Rakhshani and M. A. Mansouri-Birjandi, “Engineering Hexagonal Array of Nanoholes for High Sensitivity Biosensor and Application for Human Blood Group Detection,” vol. 17, no. 3, pp. 475–481. [Online]. Available: https://ieeexplore.ieee.org/abstract/document/8309362

[17] R. Jha and A. K. Sharma, “Design of a silicon-based plasmonic biosensor chip for human blood-group identification,” vol. 145, no. 1, pp. 200–204. [Online]. Available: https://www.sciencedirect.com/science/article/pii/S0925400509009253

[18] S. K. Raghuwanshi and P. S. Pandey, “A Numerical Study of Different Metal and Prism Choices in the Surface Plasmon Resonance Biosensor Chip for Human Blood Group Identification,” vol. 22, no. 2, pp. 292–300. [Online]. Available: https://ieeexplore.ieee.org/abstract/document/9804762

[19] P. S. Pandey, S. K. Raghuwanshi, R. Singh, and S. Kumar, “Surface Plasmon Resonance Biosensor Chip for Human Blood Groups Identification Assisted with Silver-Chromium-Hafnium Oxide,” vol. 9, no. 1, p. 21. [Online]. Available: https://www.mdpi.com/2312-7481/9/1/21

[20] H.-S. Leong, J. Guo, R. G. Lindquist, and Q. H. Liu, “Surface plasmon resonance in nanostructured metal films under the Kretschmann configuration,” vol. 106, no. 12, p. 124314. [Online]. Available: https://doi.org/10.1063/1.3273359

[21] A. A. Rifat, R. Ahmed, A. K. Yetisen, H. Butt, A. Sabouri, G. A. Mahdiraji, S. H. Yun, and F. R. M. Adikan, “Photonic crystal fiber based plasmonic sensors,” vol. 243, pp. 311–325. [Online]. Available: https://www.sciencedirect.com/science/article/pii/S0925400516319116

[22] D. Zhang, L. Men, and Q. Chen, “Microfabrication and Applications of Opto-Microfluidic Sensors,” vol. 11, no. 5, pp. 5360–5382. [Online]. Available: https://www.mdpi.com/1424-8220/11/5/5360

[23] E. K. Akowuah, T. Gorman, and S. Haxha, “Design and optimization of a novel surface plasmon resonance biosensor based on Otto configuration,” vol. 17, no. 26,

pp. 23 511–23 521. [Online]. Available: https://opg.optica.org/oe/abstract.cfm?uri=oe-17-26-23511

[24] H. R. Gwon and S. H. Lee, "Spectral and Angular Responses of Surface Plasmon Resonance Based on the Kretschmann Prism Configuration," vol. 51, no. 6, pp. 1150–1155.

[25] S. Deng, P. Wang, and X. Yu, "Phase-Sensitive Surface Plasmon Resonance Sensors: Recent Progress and Future Prospects," vol. 17, no. 12, p. 2819. [Online]. Available: https://www.mdpi.com/1424-8220/17/12/2819

[26] D. Barchiesi and A. Otto, "Excitations of surface plasmon polaritons by attenuated total reflection, revisited," vol. 36, no. 5, pp. 173–209. [Online]. Available: https://doi.org/10.1393/ncr/i2013-10088-9

[27] B. D. Gupta and R. K. Verma, "Surface Plasmon Resonance-Based Fiber Optic Sensors: Principle, Probe Designs, and Some Applications," vol. 2009, p. e979761. [Online]. Available: https://www.hindawi.com/journals/js/2009/979761/

[28] S. Singh, A. K. Sharma, P. Lohia, and D. K. Dwivedi, "Theoretical analysis of sensitivity enhancement of surface plasmon resonance biosensor with zinc oxide and blue phosphorus/MoS2 heterostructure," vol. 244, p. 167618. [Online]. Available: https://www.sciencedirect.com/science/article/pii/S0030402621012262

[29] A. Panda and P. D. Pukhrambam, "Modeling of high-performance SPR refractive index sensor employing novel 2D materials for detection of malaria pathogens," vol. 21, no. 2, pp. 312–319. [Online]. Available: https://ieeexplore.ieee.org/abstract/document/9548925/

[30] M. El-assar, T. E. Taha, F. E. A. El-Samie, H. A. Fayed, and M. H. Aly, "ZnSe-based highly-sensitive SPR biosensor for detection of different cancer cells and urine glucose levels," vol. 55, no. 1, p. 76. [Online]. Available: https://link.springer.com/10.1007/s11082-022-04326-y

[31] T. Srivastava, R. Jha, and R. Das, "High-performance bimetallic SPR sensor based on periodic-multilayer-waveguides," vol. 23, no. 20, pp. 1448–1450. [Online]. Available: https://ieeexplore.ieee.org/abstract/document/5960767/

[32] S. Singh, A. K. Sharma, P. Lohia, D. K. Dwivedi, Sadanand, H. Fouad, and M. S. Akhtar, "Sensitivity enhancement of SPR biosensor employing heterostructure blue phosphorus/MoS and silicon layer," vol. 11, no. 2, pp. 239–250. [Online]. Available: https://www.icevirtuallibrary.com/doi/10.1680/jemmr.22.00009

[33] A. Srivastava, A. Verma, R. Das, and Y. K. Prajapati, "A theoretical approach to improve the performance of SPR biosensor using MXene and black phosphorus," vol. 203, p. 163430. [Online]. Available: https://www.sciencedirect.com/science/article/pii/S0030402619313282

[34] A. Srivastava, R. Das, and Y. K. Prajapati, "Effect of Perovskite material on performance of surface plasmon resonance biosensor," vol. 14, no. 5, pp. 256–265. [Online]. Available: https://onlinelibrary.wiley.com/doi/10.1049/iet-opt.2019.0122

[35] R. K. Sonia, P. Patel, C. Prakash, C. Prakash, and D. K. Agrawal, "Low temperature synthesis and dielectric, ferroelectric and piezoelectric study of microwave sintered BaTiO3 ceramics," vol. 38, pp. 1585–1589. [Online]. Available: https://hero.epa.gov/hero/index.cfm/reference/details/reference_id/2669673

[36] R. Shukla, R. R. Kumar, D. Punetha, and S. K. Pandey, "Design perspective, fabrication, and performance analysis of formamidinium tin halide perovskite solar cell." [Online]. Available: https://ieeexplore.ieee.org/abstract/document/10043714/

[37] S. B. Desu and D. A. Payne, "Interfacial Segregation in Perovskites: III, Microstructure and Electrical Properties," vol. 73, no. 11, pp. 3407–3415. [Online]. Available: https://ceramics.onlinelibrary.wiley.com/doi/10.1111/j.1151-2916.1990.tb06468.x

[38] B. Karki, A. Uniyal, T. Sharma, A. Pal, and V. Srivastava, "Indium phosphide and black phosphorus employed surface plasmon resonance sensor for formalin detection: Numerical analysis," vol. 61, no. 1, pp. 017 101–017 101. [Online]. Available: https://

www.spiedigitallibrary.org/journals/optical-engineering/volume-61/issue-1/017101/Indium-phosphide-and-black-phosphorus-employed-surface-plasmon-resonance-sensor/10.1117/1.OE.61.1.017101.short

[39] M. Moznuzzaman, M. R. Islam, and I. Khan, "Effect of layer thickness variation on sensitivity: An SPR based sensor for formalin detection," vol. 32, p. 100419. [Online]. Available: https://www.sciencedirect.com/science/article/pii/S2214180421000246

[40] A. S. Kushwaha, A. Kumar, R. Kumar, and S. K. Srivastava, "A study of surface plasmon resonance (SPR) based biosensor with improved sensitivity," vol. 31, pp. 99–106. [Online]. Available: https://www.sciencedirect.com/science/article/pii/S1569441018300956

[41] M. Salahuddin, S. Jothilingam, M. K. Alam, A. Uniyal, and A. Pal, "Theoretical model for glucose detection in urine samples using heterogeneous layered surface plasmon resonance (SPR) sensor." [Online]. Available: https://www.researchsquare.com/article/rs-1490362/latest

[42] K. M. McPeak, S. V. Jayanti, S. J. P. Kress, S. Meyer, S. Iotti, A. Rossinelli, and D. J. Norris, "Plasmonic Films Can Easily Be Better: Rules and Recipes," vol. 2, no. 3, pp. 326–333. [Online]. Available: https://doi.org/10.1021/ph5004237

[43] A. A. Rifat, g.-i. family=RabiulHasan, given=Md., R. Ahmed, and A. E. Miroshnichenko, "Microstructured Optical Fiber-Based Plasmonic Sensors," in *Computational Photonic Sensors*, M. F. O. Hameed and S. Obayya, Eds. Springer International Publishing, pp. 203–232. [Online]. Available: https://doi.org/10.1007/978-3-319-76556-3_9

[44] M. A. Ordal, R. J. Bell, R. W. Alexander, L. L. Long, and M. R. Querry, "Optical properties of fourteen metals in the infrared and far infrared: Al, Co, Cu, Au, Fe, Pb, Mo, Ni, Pd, Pt, Ag, Ti, V, and W." vol. 24, no. 24, pp. 4493–4499. [Online]. Available: https://opg.optica.org/ao/abstract.cfm?uri=ao-24-24-4493

[45] Searching for better plasmonic materials - West - 2010 - Laser & Photonics Reviews - Wiley Online Library. [Online]. Available: https://onlinelibrary.wiley.com/doi/abs/10.1002/lpor.200900055

[46] J. Homola, "Present and future of surface plasmon resonance biosensors," vol. 377, no. 3, pp. 528–539. [Online]. Available: https://doi.org/10.1007/s00216-003-2101-0

[47] S. Bharadwaj, P. K. Maharana, R. Das, and R. Jha, "Effect of chalcogenide glass and plasmonic metal on electric field enhancement in surface plasmon resonance sensor," in *International Conference on Fibre Optics and Photonics (2012), Paper TPo.19*. Optica Publishing Group, p. TPo.19. [Online]. Available: https://opg.optica.org/abstract.cfm?uri=Photonics-2012-TPo.19

[48] B. D. Gupta and A. K. Sharma, "Sensitivity evaluation of a multi-layered surface plasmon resonance-based fiber optic sensor: A theoretical study," vol. 107, no. 1, pp. 40–46. [Online]. Available: https://www.sciencedirect.com/science/article/pii/S0925400504006719

[49] L. Han and C. Wu, "A Phase Sensitivity-Enhanced Surface Plasmon Resonance Biosensor Based on ITO-Graphene Hybrid Structure," vol. 14, no. 4, pp. 901–906. [Online]. Available: https://doi.org/10.1007/s11468-018-0872-6

[50] Y. Zhao and Y. Zhu, "Graphene-based hybrid films for plasmonic sensing," vol. 7, no. 35, pp. 14 561–14 576. [Online]. Available: https://pubs.rsc.org/en/content/articlelanding/2015/nr/c5nr03458b

[51] P. O. Patil, G. R. Pandey, A. G. Patil, V. B. Borse, P. K. Deshmukh, D. R. Patil, R. S. Tade, S. N. Nangare, Z. G. Khan, A. M. Patil, M. P. More, M. Veerapandian, and S. B. Bari, "Graphene-based nanocomposites for sensitivity enhancement of surface plasmon resonance sensor for biological and chemical sensing: A review," vol. 139, p. 111324. [Online]. Available: https://www.sciencedirect.com/science/article/pii/S0956566319303896

[52] X. Gan, H. Zhao, and X. Quan, “Two-dimensional MoS2: A promising building block for biosensors,” vol. 89, pp. 56–71. [Online]. Available: https://www.sciencedirect.com/science/article/pii/S0956566316302378

[53] A. Kumar, A. K. Yadav, A. S. Kushwaha, and S. K. Srivastava, “A comparative study among WS2, MoS2 and graphene based surface plasmon resonance (SPR) sensor,” vol. 2, no. 1, p. 100015. [Online]. Available: https://www.sciencedirect.com/science/article/pii/S2666053920300126

[54] A. Uniyal, B. Chauhan, A. Pal, and Y. Singh, “Surface plasmon biosensor based on Bi 2 Te 3 antimonene heterostructure for the detection of cancer cells,” vol. 61, no. 13, pp. 3711–3719. [Online]. Available: https://opg.optica.org/abstract.cfm?uri=ao-61-13-3711

[55] S. A. Zynio, A. V. Samoylov, E. R. Surovtseva, V. M. Mirsky, and Y. M. Shirshov, “Bimetallic layers increase sensitivity of affinity sensors based on surface plasmon resonance,” vol. 2, no. 2, pp. 62–70. [Online]. Available: https://www.mdpi.com/1424-8220/2/2/62

[56] K. Wei, X. Su, L. Zhang, P. Wu, H. Zhu, K. Wu, and Y. Guo, “Performance Evaluation of Bimetallic Surface Plasmon Resonance Biosensor Based on Copper and MXene (Ti3C2Tx).” [Online]. Available: https://www.researchsquare.com/article/rs-1569219/latest

[57] A. K. Sharma, “Simulation and analysis of Au-MgF2 structure in plasmonic sensor in near infrared spectral region,” vol. 101, pp. 491–498. [Online]. Available: https://www.sciencedirect.com/science/article/pii/S003039921731109X

[58] A. K. Pandey and A. K. Sharma, “Simulation and analysis of plasmonic sensor in NIR with fluoride glass and graphene layer,” vol. 28, pp. 94–99. [Online]. Available: https://www.sciencedirect.com/science/article/pii/S1569441017302766

[59] N. V. Suresh, K. B. Rajesh, and T. V. S. Pillai, “Sensitivity enhancement of surface plasmon resonance sensor using Al–Au–BaTiO3–Graphene layers,” vol. 50, no. 2, pp. 152–159. [Online]. Available: https://link.springer.com/10.1007/s12596-021-00694-y

[60] N. Mudgal, A. Saharia, K. K. Choure, A. Agarwal, and G. Singh, "Sensitivity enhancement with anti-reflection coating of silicon nitride (Si3N4) layer in silver-based Surface Plasmon Resonance (SPR) sensor for sensing of DNA hybridization," vol. 126, no. 12, p. 946. [Online]. Available: https://doi.org/10.1007/s00339-020-04126-9

[61] Shivangani, P. Lohia, P. K. Singh, S. Singh, and D. K. Dwivedi, "Design and modeling of reconfigurable surface plasmon resonance refractive index sensor using Al2O3, nickel, and heterostructure BlueP/WSe2 nanofilms," vol. 52, no. 3, pp. 1358–1369. [Online]. Available: https://link.springer.com/10.1007/s12596-022-00973-2

[62] Y. Vasimalla and H. S. Pradhan, "A highly performed SPR biosensor based on bismuth ferrite-bromide materials-BP/graphene hybrid structure," vol. 53, no. 12, p. 695. [Online]. Available: https://doi.org/10.1007/s11082-021-03347-3

[63] S. Singh, S. Singh, P. K. Singh, R. K. Yadav, P. Lohia, and D. K. Dwivedi, "Theoretical Study of Malaria Detection in Blood Samples Using Bimetal Layer and Zinc Telluride Nanomaterial-Based Surface Plasmon Resonance Biosensor," vol. 18, no. 6, pp. 2125–2136. [Online]. Available: https://link.springer.com/10.1007/s11468-023-01913-x

[64] H. H. Li, "Refractive index of ZnS, ZnSe, and ZnTe and its wavelength and temperature derivatives," vol. 13, no. 1, pp. 103–150. [Online]. Available: https://pubs.aip.org/aip/jpr/article-abstract/13/1/103/241325

[65] D. T. F. Marple, "Refractive index of znse, znte, and cdte," vol. 35, no. 3, pp. 539–542. [Online]. Available: https://pubs.aip.org/aip/jap/article-abstract/35/3/539/147171

[66] H. Li, L. Lin, and S. Xie, "Refractive index of human whole blood with different types in the visible and near-infrared ranges," in *Laser-Tissue Interaction XI: Photochemical, Photothermal, and Photomechanical*, vol. 3914. SPIE, pp. 517–521. [Online]. Available: https://www.spiedigitallibrary.org/conference-proceedings-of-spie/3914/0000/Refractive-index-of-human-whole-blood-with-different-types-in/10.1117/12.388073.short

[67] B. Dey, M. S. Islam, and J. Park, “Numerical design of high-performance WS2/metal/WS2/graphene heterostructure based surface plasmon resonance refractive index sensor,” vol. 23, p. 104021. [Online]. Available: https://www.sciencedirect.com/science/article/pii/S2211379721001881

[68] P. S. Pandey, S. K. Raghuwanshi, R. Singh, and S. Kumar, “Surface plasmon resonance biosensor chip for human blood groups identification assisted with silver-chromium-hafnium oxide,” vol. 9, no. 1, p. 21. [Online]. Available: https://www.mdpi.com/2312-7481/9/1/21

[69] S. K. Raghuwanshi and P. S. Pandey, “A numerical study of different metal and prism choices in the surface plasmon resonance biosensor chip for human blood group identification,” vol. 22, no. 2, pp. 292–300. [Online]. Available: https://ieeexplore.ieee.org/abstract/document/9804762/